

Penalized Generative Variable Selection

Tong Wang* Jian Huang † Shuangge Ma ‡

Abstract

Deep networks are increasingly applied to a wide variety of data, including data with high-dimensional predictors. In such analysis, variable selection can be needed along with estimation/model building. Many of the existing deep network studies that incorporate variable selection have been limited to methodological and numerical developments. In this study, we consider modeling/estimation using the conditional Wasserstein Generative Adversarial networks. Group Lasso penalization is applied for variable selection, which may improve model estimation/prediction, interpretability, stability, etc. Significantly advancing from the existing literature, the analysis of censored survival data is also considered. We establish the convergence rate for variable selection while considering the approximation error, and obtain a more efficient distribution estimation. Simulations and the analysis of real experimental data demonstrate satisfactory practical utility of the proposed analysis.

Keywords: Conditional Wasserstein Generative Adversarial Networks; Penalized variable selection; Consistency.

*Department of Biostatistics, Yale School of Public Health, New Haven, Connecticut, USA

†Department of Applied Mathematics, The Hong Kong Polytechnic University, Hong Kong SAR, China

‡Department of Biostatistics, Yale School of Public Health, New Haven, Connecticut, USA

1 Introduction

In data analysis, an essential task is to establish the relationship between a response Y and predictors \mathbf{X} . Numerous regression techniques have been developed for this. It has been increasingly recognized that regression sometimes can be too rigid, and over the past decade, we have witnessed a surge in deep network techniques, which have demonstrated great power in a wide range of domains, such as computer vision, speech recognition, biomedical diagnosis, natural language processing, and others. “Traditional” deep networks have often been criticized for being “black-boxes” with somewhat limited statistical principles, theoretical guarantees, and interpretability.

The fast development of data collection techniques in many domains has made the analysis of data with high-dimensional predictors routine. With such data, model sparsity is often assumed, under which only a subset of the predictors is relevant. For many specific problems, this assumption has been suggested as sensible. Accordingly, variable selection has been conducted, which can lead to more reliable, interpretable, and efficient estimation. Under the regression framework, various penalization techniques have been developed and shown to have satisfactory theoretical and numerical properties (Zou and Hastie, 2005; Liu et al., 2007; Zhang, 2010). Alternative selection techniques include Bayesian, thresholding, boosting, and others.

Deep network techniques are now increasingly applied to data with high-dimensional predictors. A natural question is whether variable selection can be incorporated in such analysis. Compared to their regression counterparts, deep networks have more complicated model structures and many more parameters, leading to a stronger demand for variable selection. Here it is first noted that some pruning techniques, such as random dropout, can generate sparser networks but cannot conduct variable selection. In the literature,

there have been a few efforts. For example, one strategy is to conduct variable selection via constructing a sparse network. With imaging data, Zhao et al. (2015) and Scardapane et al. (2017) applied group Lasso penalization to either a specific module or the entire network. Feng and Simon (2017); Dinh and Ho (2020) and Luo and Halabi (2023) studied the sparse input neural network and developed the corresponding algorithms. Lemhadri et al. (2021) developed LassoNet by adding a skip (residual) layer, which can control the participation of a feature in any hidden layer. As an alternative strategy, researchers have developed new network architectures for variable selection. For example, Li et al. (2016) performed selection by adding a sparse one-to-one layer to networks, and Chen et al. (2021) established its selection consistency under some conditions with a greedy algorithm they proposed. Lu et al. (2018) designed a new deep neural network architecture by integrating knockoff filters to achieve feature selection with a controlled false discovery rate. Liang et al. (2018) developed a neural network variable selection method under the Bayesian paradigm.

The aforementioned and other studies have demonstrated promising performance of deep networks, without and with variable selection. Many of them have been limited to methodological and numerical developments, while insufficient theoretical guarantee has been provided. Nevertheless, theoretical investigation has been conducted in a handful of studies. For example, when variable selection is not incorporated, convergence properties of the ReLU neural networks have been studied under least squares regression (Bauer and Kohler, 2019; Schmidt-Hieber, 2020), quantile regression (Padilla et al., 2020), robust non-parametric regression (Shen et al., 2021), and a general class of nonparametric regression-type loss functions (Farrell et al., 2021). Effort has also been made when variable selection is incorporated. Sun et al. (2022) established selection consistency for Bayesian sparse deep neural networks based on marginal posterior inclusion probabilities. Chen et al. (2021) established selection consistency with approximation error for the network with a one-to-one

selection layer under a regression framework. The aforementioned and some other studies have examined selection consistency with respect to certain specifically designed network architectures (and hence may not be generalizable). There are also studies on the commonly adopted fully connected networks. For example, Feng and Simon (2017) examined variable selection consistency for single-layer neural networks. Additionally, Dinh and Ho (2020) examined selection properties from a parametric perspective through setting the underlying regression function as the neural network.

The goal of this study is to further advance the research on variable selection with deep networks. This study is connected to but also significantly differs from the existing literature in multiple important aspects. Specifically, to more comprehensively describe the response-predictor relationship, we consider the Wasserstein generative adversarial network (WGAN), which significantly differ from the networks that are limited to certain specific quantities such as conditional mean. It makes milder assumptions on data structures and can be more suitable for modeling complex and unknown relationships. For variable selection, we adopt penalization, which has been demonstrated as effective in multiple studies. Different from some studies that have an additional sparse layer, group penalization is imposed to the first-layer weights. Additionally, there are multiple notable differences in the statistical development. For example, we consider deep neural networks whose width and depth can increase with sample size – this significantly differs from those studies with fixed networks. Different from Dinh and Ho (2020) and some others, no assumption is imposed on the underlying regression function, making the proposed networks more flexible. Approximation error, which has a crucial role in nonparametric estimation but has been ignored in Feng and Simon (2017); Dinh and Ho (2020) and some other studies, is taken into consideration. Most of the existing studies, in particular those incorporating variable selection, have been limited to continuous and categorical responses. This study further

advances by also considering censored survival data. Overall, this study can deliver a practically useful tool with a strong statistical ground, advancing deep network methodological and theoretical research.

2 Methods

Let $\mathcal{A} = \{(\mathbf{x}_i, y_i) : i = 1, \dots, n\}$ denote a dataset of n i.i.d. observations, where the predictor $\mathbf{x}_i \in \mathbb{R}^p$ and the response $y_i \in \mathbb{R}$. To mitigate data-induced correlations, we split \mathcal{A} into two subsets: $\mathcal{A}_1 = \{(\mathbf{x}_i, y_i) : i = 1, \dots, n_1\}$ and $\mathcal{A}_2 = \{(\mathbf{x}_i, y_i) : i = n_1 + 1, \dots, n_1 + n_2\}$ with $n_1 + n_2 = n$.

2.1 Penalized WGAN

The proposed analysis consists of two stages/steps. In both stages, we adopt WGAN to describe the response-predictor relationship. Compared to those focused on certain specific quantities (for example, conditional mean), GWAN is built on distributions and can more comprehensively measure model fitting. Its advantages have been increasingly recognized in the recent literature. In the first stage, the first subset of data is analyzed, and the main goal is to identify the predictors that are important for the response. Penalization is applied for variable selection. In the second stage, the second subset of data is analyzed. With only the selected variables, a refined estimation is conducted. Here no variable selection is needed, and hence penalization is not imposed.

Stage 1 WGAN corresponds to a minimax two-player game, and two networks are involved in training: a generator network g_{θ_1} with predictors \mathbf{x} and a noise vector \mathbf{z} as the input, and a discriminator network f_{ϕ_1} with (\mathbf{x}, y) as the input, where θ_1 and ϕ_1 are the network parameters (weights and biases). We denote the first-layer weights in g_{θ_1} by $\mathbf{w}_0(\theta_1) \in$

$\mathbb{R}^{p_1 \times (p+m)}$, where p_1 is the width of the first hidden layer and m is the dimension of \mathbf{z} , which is generated from the standard normal distribution (noting that some other distributions are also applicable).

Using only \mathcal{A}_1 , we propose the penalized objective function:

$$l_1(g_{\theta_1}, f_{\phi_1}) = \frac{1}{n_1} \sum_{i=1}^{n_1} f_{\phi_1}(\mathbf{x}_i, g_{\theta_1}(\mathbf{x}_i, \mathbf{z}_i)) - \frac{1}{n_1} \sum_{i=1}^{n_1} f_{\phi_1}(\mathbf{x}_i, y_i) + \lambda_n \sum_{j=1}^p \|\mathbf{w}_0(\theta_1)^{[j]}\|_2, \quad (1)$$

where λ_n is a data-dependent tuning parameter and $\mathbf{w}_0(\theta_1)^{[j]}$ is the j -th column of $\mathbf{w}_0(\theta_1)$, which connects the j -th component of input \mathbf{x}_i . The proposed estimation is defined as:

$$(\hat{\theta}_1, \hat{\phi}_1) = \arg \min_{\theta_1} \max_{\phi_1} l_1(g_{\theta_1}, f_{\phi_1}). \quad (2)$$

With the estimated weights, the network structures can be obtained. The input variables with the estimated first-layer weights being nonzero are identified as important for the response – this is consistent with penalized regression and some existing penalized deep network selection studies. Overall, the proposed training process is sketched in Figure 1.

Rationale The first two terms in (1) empirically measure the 1-Wasserstein distance between the joint distributions of $(X, g_{\theta_1}(\mathbf{X}, \mathbf{Z}))$ and (\mathbf{X}, Y) , denoted by $P_{\mathbf{X}, g_{\theta_1}}$ and $P_{\mathbf{X}, Y}$, respectively. It can be seen from (2), training a WGAN amounts to finding the Nash equilibrium between g_{θ_1} and f_{ϕ_1} , with g_{θ_1} mimicking $P_{Y|\mathbf{X}}$ and f_{ϕ_1} discriminating the difference between $P_{\mathbf{X}, g_{\theta_1}}$ and $P_{\mathbf{X}, Y}$. The minimum of this distance is achieved when $P_{\mathbf{X}, g_{\theta_1}}$ and $P_{\mathbf{X}, Y}$ are identical, which indicates that $g_{\theta_1}(\mathbf{x}, \mathbf{Z})$ follows the conditional distribution of Y given $\mathbf{X} = \mathbf{x}$.

The last term in (1) is a group Lasso penalty, designed for identifying important input variables. Penalization has been adopted in multiple deep network studies for variable

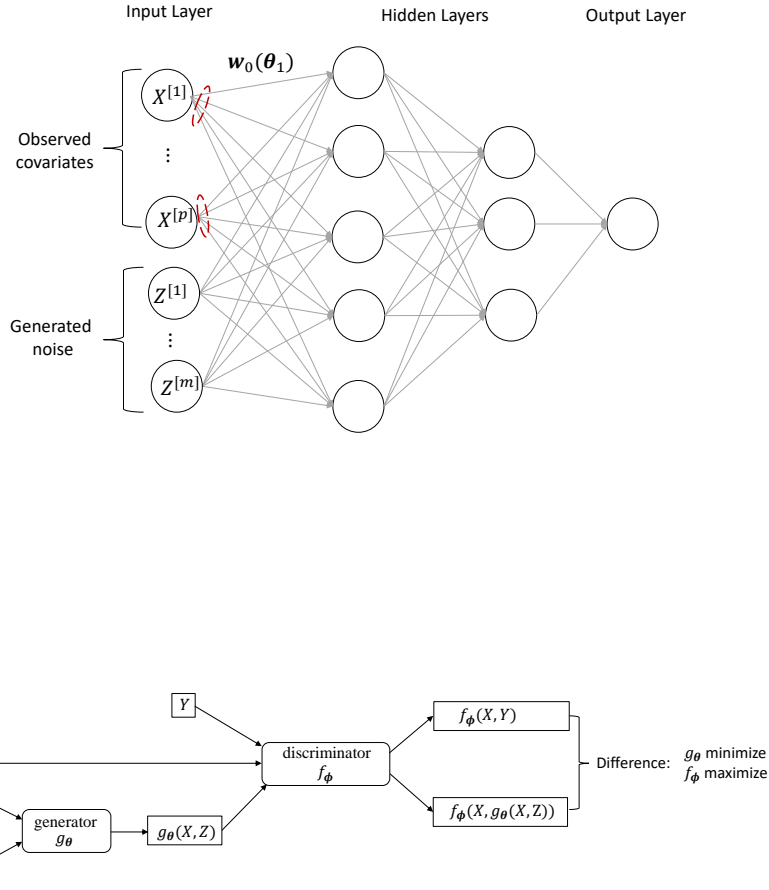


Figure 1: Upper: Architecture of the penalized generator network g_{θ_1} . Lower: Training process of the proposed method.

selection. Although sharing a similar spirit, different studies have different penalization designs. Here, the adopted penalty treats all the first-layer weights corresponding to an input variable as a group. With its all-in-or-all-out property, if a group is estimated as zero, the corresponding variable can be dropped from the model. This cannot be achieved using for example Lasso. On the other hand, if a group is estimated as nonzero, the corresponding input variable has all the first-layer weights nonzero, allowing for sufficient contributions. This strategy differs from that involving an additional sparse layer. Our

preliminary examination does not suggest the dominance of one strategy over the other. As group penalization is adopted for the purpose of variable selection, it is only applied to the first layer of g_{θ_1} . Some published studies have also imposed penalization to the other layers to regularize estimation and/or achieve sparsity. If desirable, this can be coupled with the proposed approach too.

Stage 2 To further refine estimation, network retraining is conducted using only the identified important input variables. Such retraining has been commonly conducted with penalized regression. Denote $\hat{\mathbf{X}}^s$. With the low dimensionality of $\hat{\mathbf{X}}^s$ and the focus on estimation, no penalization is imposed in this stage. Using \mathcal{A}_2 only, we consider the un-penalized objective function:

$$l_2(g_{\theta_2}, f_{\phi_2}) = \frac{1}{n_2} \sum_{i=1}^{n_2} f_{\phi_2}(\tilde{\mathbf{x}}_{n_1+i}^s, g_{\theta_2}(\tilde{\mathbf{x}}_{n_1+i}^s, \mathbf{z}_i)) - \frac{1}{n_2} \sum_{i=1}^{n_2} f_{\phi_2}(\tilde{\mathbf{x}}_{n_1+i}^s, y_{n_1+i}). \quad (3)$$

where g_{θ_2} and f_{ϕ_2} are a generator network and a discriminator network with parameters θ_2 and ϕ_2 , respectively. The proposed estimation is defined as: $(\hat{\theta}_2, \hat{\phi}_2) = \arg \min_{\theta_2} \max_{\phi_2} l_2(g_{\theta_2}, f_{\phi_2})$.

Remark 1. *Splitting data leads to a reduction in sample size. In principle, it is possible to use the whole dataset for both stages. However, this may make theoretical development much more challenging. Similar data splitting has been adopted in multiple published studies.*

2.2 Implementation

Here, we present the implementation details including the network architecture and the computational algorithm. Throughout this article, we consider the feedforward neural network (FNN), which can be expressed as a composition of a series of functions:

$$\zeta(\mathbf{x}) = \mathbf{w}_{\mathcal{L}} \sigma(\mathbf{w}_{\mathcal{L}-1} \sigma(\dots \mathbf{w}_1 \sigma(\mathbf{w}_0 \mathbf{x} + \mathbf{b}_0) + \mathbf{b}_1) + \dots) + \mathbf{b}_{\mathcal{L}-1}) + \mathbf{b}_{\mathcal{L}}, \quad \mathbf{x} \in \mathbb{R}^{p_0}.$$

Here $\sigma(\cdot)$ is the activation function, \mathcal{L} is depth of the network, p_0 is the dimension of the input vector, p_i is the width of the i -th layer for $i = 1, \dots, \mathcal{L}$, and $\mathbf{w}_i \in \mathbb{R}^{p_{i+1} \times p_i}$ and $\mathbf{b}_i \in \mathbb{R}^{p_{i+1}}$ are the weight matrix and bias vector of the i -th layer, respectively. The width of $\zeta(\cdot)$ is described as $\mathcal{W} = \max\{p_1, \dots, p_{\mathcal{L}}\}$.

To emphasize penalization in the objective function, the first-layer weights of the generator network g_{θ_1} are denoted by $\mathbf{w}_0(\theta_1)$. $\mathbf{w}_0(\theta_1) \in \mathbb{R}^{p_1 \times (p+m)}$ includes two parts: the first p columns connecting the predictors \mathbf{X} and the rest connecting the generated noise \mathbf{Z} . Algorithm 1 presents the most essential component of the computation. Weight clipping is applied during the training of the discriminator network f_{ϕ_1} to satisfy the Lipschitz constraint required by the Wasserstein distance. Although Gulrajani et al. (2017) showed that a gradient penalty can enforce this Lipschitz constraint better in training WGANs, weight clipping performs comparably and is computationally easier for the present problem. The second step computation is omitted as it is a simplified version of Algorithm 1.

Algorithm 1 Penalized WGAN

Require: Tuning parameter λ_n ; Minibatch size $n_b \leq n_1$; Clipping parameter c ; Noise dimension m ; Learning rates r_f, r_g .

- 1: **for** number of training iterations in stage 1 **do**
- 2: Sample $\{(\mathbf{x}_{bj}, y_{bj})\}_{j=1}^{n_b}$ from $\{(\mathbf{x}_i, y_i)\}_{i=1}^{n_1}$, and $\{\mathbf{z}_j\}_{j=1}^{n_b}$ from $N(\mathbf{0}, \mathbf{I}_m)$.
- 3: Update the discriminator f_{ϕ_1} by ascending its stochastic gradient:

$$f_{\phi_1} \leftarrow \nabla_{\phi_1} \left[\frac{1}{n_b} \sum_{j=1}^{n_b} f_{\phi_1}(\mathbf{x}_{bj}, g_{\theta_1}(\mathbf{x}_{bj}, \mathbf{z}_j)) - \frac{1}{n_b} \sum_{j=1}^{n_b} f_{\phi_1}(\mathbf{x}_{bj}, y_{bj}) \right],$$

$$\phi_1 \leftarrow \phi_1 + r_f \cdot \text{RMSPProp}(\phi_1, f_{\phi_1}), \quad \phi_1 \leftarrow \text{clip}(\phi_1, -c, c).$$

- 4: Update the generator g_{θ_1} by descending its stochastic gradient:

$$g_{\theta_1} \leftarrow \nabla_{\theta} \left[\frac{1}{n_b} \sum_{j=1}^{n_b} f_{\phi}(\mathbf{x}_{bj}, g_{\theta}(\mathbf{x}_{bj}, \mathbf{z}_j)) + \lambda_n \sum_{l=1}^p \|\mathbf{w}_0(\theta_1)^{[l]}\|_2 \right],$$

$$\theta_1 \leftarrow \theta_1 - r_g \cdot \text{RMSPProp}(\theta, g_{\theta_1}).$$

- 5: **end for**
-

3 Statistical Properties

3.1 Definition of importance

Let $Y \in \mathcal{Y} \subseteq \mathbb{R}$ and $\mathbf{X} \in \mathcal{X} \subseteq \mathbb{R}^p$. Since the conditional distribution $P_{Y|\mathbf{X}}$ can fully describe the relationship between \mathbf{X} and Y , it is natural to define the important variables as the subset of \mathbf{X} that $P_{Y|\mathbf{X}}$ only depends on.

Definition 1 (Importance). *Let $\mathbf{X}^{[j]}$ be the j -th component of \mathbf{X} . Then, $\mathbf{X}^{[j]}$ is defined as unimportant if and only if*

$$P_{Y|\mathbf{X}^{[-j]=\mathbf{x}^{[-j]}}} \sim P_{Y|\mathbf{X}=\mathbf{x}}, \quad \forall \mathbf{x} \in \mathcal{X}, \quad (4)$$

where $\mathbf{X}^{[-j]} = (X^{[1]}, \dots, X^{[j-1]}, X^{[j+1]}, \dots, X^{[p]})$ and $\mathbf{x}^{[-j]} = (x^{[1]}, \dots, x^{[j-1]}, x^{[j+1]}, \dots, x^{[p]})$, and “ \sim ” means the equivalence of two distributions.

We separate \mathbf{X} into $\mathbf{X}^s \in \mathbb{R}^{p_s}$ and $\mathbf{X}^c \in \mathbb{R}^{p_c}$, with $p_s + p_c = p$, denoting the important and unimportant variables, respectively. Without loss of generality, assume that the first p_s components of \mathbf{X} are important. For any $\mathbf{x} \in \mathbf{X}$, $P_{Y|\mathbf{X}=\mathbf{x}} \sim P_{Y|\mathbf{X}^s=\mathbf{x}^s}$. Note that this definition of importance allows for correlations among the predictors. It is a general definition of sparsity and fits many commonly adopted models. For example, for the mean regression model, $\mathbf{X}^{[j]}$ is unimportant if and only if $\mathbb{E}[Y|\mathbf{X}^{[j]}] = \mathbb{E}[Y|\mathbf{X}]$. For the quantile regression model, $\mathbf{X}^{[j]}$ is unimportant at a particular quantile level τ if and only if $Q_{Y|\mathbf{X}^{[j]}}(\tau) = Q_{Y|\mathbf{X}}(\tau)$. For the Cox regression model, $\mathbf{X}^{[j]}$ is unimportant if and only if the hazard function $\lambda(Y|\mathbf{X}^{[j]}) = \lambda(Y|\mathbf{X})$. Definition 1 is a sufficient condition for all the above.

3.2 Connection between the important variables and target parameters

To identify the important subset \mathbf{X}^s , we aim to estimate a function $g(\mathbf{X} = \mathbf{x}, \mathbf{Z})$ which follows $P_{Y|\mathbf{X}=\mathbf{x}}$ for any $\mathbf{x} \in \mathcal{X}$, where \mathbf{Z} is a known random vector. The noise-outsourcing lemma (Kallenberg, 2002) guarantees the existence of such a function $g(\mathbf{X}, \mathbf{Z})$, as long as \mathcal{Y} is a standard Borel space and $\mathbf{Z} \in \mathcal{Z} \subseteq \mathbb{R}^m$ is an independent m -dimensional noise vector sampled from $N(\mathbf{0}, \mathbf{I}_m)$ with $m \geq 1$. Motivated by Liu et al. (2021), the estimation of g can be achieved through matching $P_{\mathbf{X},g}$ and $P_{\mathbf{X},Y}$ using the dual form of the 1-Wasserstein distance (Villani, 2009):

$$W(P_{\mathbf{X},g}, P_{\mathbf{X},Y}) = \sup_{f \in \mathcal{F}_{\text{Lip}}^1} \{ \mathbb{E}_{\mathbf{X},\mathbf{Z}} f(\mathbf{X}, g(\mathbf{X}, \mathbf{Z})) - \mathbb{E}_{\mathbf{X},Y} f(\mathbf{X}, Y) \}. \quad (5)$$

where $\mathcal{F}_{\text{Lip}}^1$ is the 1-Lipschitz function class. Let g^* be the minimizer of $W(P_{\mathbf{X},g}, P_{\mathbf{X},Y})$ over the Borel space, so that $W(P_{\mathbf{X},g^*}, P_{\mathbf{X},Y}) = 0$. g^* satisfies

$$g^*(\mathbf{x}, \mathbf{Z}) \sim P_{Y|\mathbf{X}=\mathbf{x}}, \forall \mathbf{x} \in \mathcal{X}, \quad (6)$$

as it is the sufficient and necessary condition for $W(P_{\mathbf{X},g}, P_{\mathbf{X},Y}) = 0$. Together with (6) and Definition 1, $g^*(\mathbf{X}, \mathbf{Z})$ depends on \mathbf{X}^s only. We construct an estimator of g^* within a function class consisting of feedforward neural networks, denoted by \mathcal{G}_{θ_1} with network parameter θ_1 . To simplify presentation, we divide the first-layer weights of g_{θ_1} into three parts:

$$\mathbf{w}_0(\theta_1) = (\boldsymbol{\mu}_1, \boldsymbol{\nu}_1, \mathbf{v}_1), \quad (7)$$

where $\boldsymbol{\mu}_1 \in \mathbb{R}^{p_1 \times p_s}$ connects \mathbf{X}^s , $\boldsymbol{\nu}_1 \in \mathbb{R}^{p_1 \times p_c}$ connects \mathbf{X}^c , and $\boldsymbol{v}_1 \in \mathbb{R}^{p_1 \times m}$ connects \mathbf{Z} .

Then, referring to the optimal network solution $g_{\boldsymbol{\theta}_1^*} \in \arg \min_{g_{\boldsymbol{\theta}_1} \in \mathcal{G}_{\boldsymbol{\theta}_1}} W(P_{\mathbf{X}, g_{\boldsymbol{\theta}_1}}, P_{\mathbf{X}, Y})$, we define a set of $\boldsymbol{\theta}$ as

$$\Theta = \{\boldsymbol{\theta}, W(P_{\mathbf{X}, g_{\boldsymbol{\theta}_1}(\mathbf{X}, \mathbf{Z})}, P_{\mathbf{X}, Y}) = W(P_{\mathbf{X}, g_{\boldsymbol{\theta}_1^*}(\mathbf{X}, \mathbf{Z})}, P_{\mathbf{X}, Y})\}. \quad (8)$$

With proper conditions on the data structure and network class, $g_{\boldsymbol{\theta}_1^*}$ can approach g^* close enough such that, within $g_{\boldsymbol{\theta}_1^*}$'s first-layer, the sub-components connecting \mathbf{X}^s are non-zero, and those connecting \mathbf{X}^c are zero. Then, for any $\boldsymbol{\theta} \in \Theta$ with first-layer weights $\boldsymbol{w}_0(\boldsymbol{\theta}) = (\boldsymbol{\mu}, \boldsymbol{\nu}, \boldsymbol{v})$, there exists a positive constant $c_\mu > 0$ such that $\min_{1 \leq j \leq p_s} \|\boldsymbol{\mu}^{[j]}\|_2 \geq c_\mu$. Further, if we set $\boldsymbol{\nu} = \mathbf{0}$, $\boldsymbol{\theta} \in \Theta$ still holds. These properties of $g_{\boldsymbol{\theta}_1^*}$ and Θ are given in Lemmas 5-6 in Appendix.

In practice, the distribution of (\mathbf{X}, Y) is unknown, and the network parameter $\hat{\boldsymbol{\theta}}_1$ obtained in (2) lies outside of Θ . To measure the distance between $\boldsymbol{\theta}$ and Θ , we define metric $d(\boldsymbol{\theta}, \Theta)$:

$$d(\boldsymbol{\theta}, \Theta) := \min_{\boldsymbol{\vartheta} \in \Theta} \|\boldsymbol{\theta} - \boldsymbol{\vartheta}\|_2, \quad (9)$$

where $\|\cdot\|_2$ is the Euclidean norm. Subsequently, $d(\hat{\boldsymbol{\theta}}_1, \Theta) \rightarrow 0$ is sufficient for $\hat{\boldsymbol{\mu}}$ to be bounded away from zero. Thus, we can obtain the selection results via establishing the convergence rate of the proposed penalized generator network $g_{\hat{\boldsymbol{\theta}}_1}$ in terms of its parameters.

3.3 Convergence rate

Here, we describe the main theoretical results. The assumed conditions and detailed proofs are provided in Appendix. In what follows, the asymptotic notation $A \lesssim B$ means that

$A \leq CB$ for some constant $C > 0$.

Theorem 1. *Suppose that Conditions 1-6 hold. If $p = o(\log^c n_1)$ with $0 < c < 1$ and $\lambda_n = O(n_1^{-\frac{1}{2(p+1)}})$, $\hat{\boldsymbol{\theta}}_1$ defined in (2) with first-layer weights $\mathbf{w}_0(\hat{\boldsymbol{\theta}}_1) = (\hat{\boldsymbol{\mu}}_1, \hat{\boldsymbol{\nu}}_1, \hat{\boldsymbol{v}}_1)$ satisfies*

$$\mathbb{E}[d(\hat{\boldsymbol{\theta}}_1, \Theta)] \lesssim \left(n_1^{-\frac{1}{p+1}} \log n_1\right)^{\frac{1}{2(a-1)}}, \quad \mathbb{E}\|\hat{\boldsymbol{\nu}}_1\|_2 \lesssim n_1^{-\frac{1}{2(a-1)(p+1)}} \log n_1,$$

where $a > 2$ is a positive constant, and \mathbb{E} is taken with respect to $\{(\mathbf{X}_i, Y_i)\}_{i=1}^{n_1}$ and $\{\mathbf{Z}_i\}_{i=1}^{n_1}$.

Corollary 1. *Suppose that Conditions 1-6 hold. If p is fixed and $\lambda_n = O(n_1^{-\frac{1}{2(p+1)}})$, there exists a positive constant $a > 2$ such that*

$$\mathbb{E}[d(\hat{\boldsymbol{\theta}}_1, \Theta)] \lesssim \left(\frac{\log n_1}{n_1}\right)^{\frac{1}{2(p+1)(a-1)}}, \quad \mathbb{E}\|\hat{\boldsymbol{\nu}}_1\|_2 \lesssim \left(\frac{\log n_1}{n_1}\right)^{\frac{1}{2(p+1)(a-1)}}.$$

In the establishment of the convergence rate, Theorem 1 is more general, while Corollary 1 is more specific to the case of a finite p . They show that $\mathbb{E}[d(\hat{\boldsymbol{\theta}}_1, \Theta)] \rightarrow 0$, which leads to that the important variables can be identified with a high probability. It is noted that the convergence rate does not depend on m .

Corollary 2. *Suppose that Conditions 1-6 hold. If $p = o(\log^c n_1)$ with $c \in (0, 1)$ and $\lambda_n = O(n_1^{-\frac{1}{2(p+1)}})$, there exists a positive threshold c_{p_s} depending on p_s such that, for any $j = 1, \dots, p_s$ and $k = 1, \dots, p_c$,*

$$\Pr(\{\|\hat{\boldsymbol{\mu}}_1^{[j]}\|_2 \geq c_{p_s}\} \cap \{\|\hat{\boldsymbol{\nu}}_1^{[k]}\|_2 \leq c_{p_s}\}) \rightarrow 1.$$

Define the empirically selected variables as $\hat{\mathbf{X}}^s = \{\mathbf{X}^{[j]} : \|\mathbf{w}_0(\hat{\boldsymbol{\theta}}_1)^{[j]}\|_2 \geq c_{p_s}, j = 1, \dots, p\}$. Corollary 2 suggests that there exists a threshold with which the penalized WGAN can select a model that only involves the important variables with probability

converging to 1. Then, the convergence rate of the second stage generator network $g_{\hat{\theta}_2}$ can be established in term of the Wasserstein distance.

Theorem 2. *Suppose that Conditions 1-6 hold. If $p = o(\log^c n_1)$ with $c \in (0, 1)$ and $\lambda_n = O(n_1^{-\frac{1}{2(p+1)}})$, then with probability $1 - c_{p_s} n_1^{-\frac{1}{2(a-1)(p+1)}} \log n_1$,*

$$\mathbb{E}W(P_{\hat{\mathbf{X}}^s, g_{\hat{\theta}_2}}, P_{\mathbf{X}^s, Y}) \lesssim n_2^{-\frac{2}{p_s+1}} \log n_2, \quad (10)$$

where c_{p_s} is a positive constant depending on p_s .

4 Accommodating survival data

Here, we extend the proposed approach to accommodate right censored survival response. Relatively, development of deep networks for survival data has been limited, especially under the WGAN framework and/or when variable selection is needed.

Let T be the event time and C be the censoring time. We observe (Y, Δ) , where $Y = \min(T, C)$, $\Delta = \mathbb{1}(T \leq C)$, and $\mathbb{1}(\cdot)$ is the indicator function. Let $\mathbf{X} \in \mathcal{X} \subset \mathbb{R}^p$ be the p -dimensional predictor vector. Coherent with the above methodological development, we propose the penalized objective function at the population level as:

$$L(g_{\theta_1}, f_{\phi_1}) = \mathbb{E}_{\mathbf{X}, \mathbf{Z}} f_{\phi_1}(\mathbf{X}, g_{\theta_1}(\mathbf{X}, \mathbf{Z})) - \mathbb{E}_{\mathbf{X}, T} f_{\phi_1}(\mathbf{X}, T) + \lambda_n \sum_{j=1}^p \left\| \mathbf{w}_0(\theta_1)^{[j]} \right\|_2. \quad (11)$$

The next step is to construct the corresponding empirical objective function based on the observed censored data (\mathbf{X}, Y, Δ) , for which we resort to the Kaplan-Meier weighting.

Consider a random sample $\{(\mathbf{x}_i, y_i, \Delta_i), i = 1, \dots, n\}$. Studies such as Stute (1996) suggest that the joint distribution function of (\mathbf{X}, T) , denoted by $F_{\mathbf{X}, T}$, can be consistently

estimated using the Kaplan-Meier estimator $\hat{F}_{\mathbf{X},T}$ defined as:

$$\hat{F}_{\mathbf{X},T}(\mathbf{X}, Y) = \sum_{i=1}^n \omega_{(i)} \mathbb{1}\{\mathbf{X}_{(i)} \leq \mathbf{x}, Y_{(i)} \leq y\}, \quad (12)$$

where $Y_{(1)} \leq \dots \leq Y_{(n)}$ are the order statistics of Y_i 's, $\mathbf{X}_{(1)}, \dots, \mathbf{X}_{(n)}$ are the associated predictors, and $\omega_{(i)}$'s are the jumps in the Kaplan-Meier estimator and can be computed as:

$$\omega_{(1)} = \frac{\Delta_{(1)}}{n}, \quad \omega_{(i)} = \frac{\Delta_{(i)}}{n-i+1} \prod_{j=1}^{i-1} \left(\frac{n-j}{n-j+1} \right)^{\Delta_{(j)}}, \quad i = 2, \dots, n.$$

Here $\Delta_{(1)}, \dots, \Delta_{(n)}$ are the associated indicators of the ordered Y_i 's. Accordingly, the empirical version of (11) is:

$$l_1(g_{\theta_1}, f_{\phi_1}) = \frac{1}{n_1} \sum_{i=1}^{n_1} f_{\phi_1}(\mathbf{x}_i, g_{\theta_1}(\mathbf{x}_i, \mathbf{z}_i)) - \sum_{i=1}^{n_1} \omega_{(i)} f_{\phi_1}(\mathbf{x}_{(i)}, y_{(i)}) + \lambda_n \sum_{j=1}^d \left\| \mathbf{w}_0(\theta_1)^{[i,j]} \right\|_2, \quad (13)$$

where $\mathbb{E}_{\mathbf{X},T} f_{\phi_1}(\mathbf{X}, T)$ is estimated by the $\omega_{(n_i)}$ -weighted mean. Here notations have similar implications as in the previous section. The identification of the important input variables can be conducted in the same manner as above.

In the second stage of network retraining, we consider the objective function:

$$l_2(g_{\theta_2}, f_{\phi_2}) = \frac{1}{n_2} \sum_{i=1}^{n_2} f_{\phi_2}(\hat{\mathbf{x}}_{n_1+i}^s, g_{\theta_2}(\hat{\mathbf{x}}_{n_1+i}^s, \mathbf{z}_i)) - \sum_{i=1}^{n_2} \omega_{(i)} f_{\phi_2}(\hat{\mathbf{x}}_{n_1+i}^s, y_{n_1+i}).$$

The training process is slightly different from the previous section. Details are provided in Algorithm 2 in Appendix.

To establish convergence rate as in Section 3, we first establish Proposition 1 to provide

the upper bound of the Kaplan-Meier estimator $\hat{F}_{\mathbf{X},T}$ and the distribution of interest $F_{\mathbf{X},T}$ in terms of the 1-Wasserstein distance.

Proposition 1. *Suppose that Conditions 7-8 hold and that (\mathbf{X}, T) satisfies Condition 1.*

Let $\hat{F}_{\mathbf{X},T}(\mathbf{x}, t) = \sum_{i=1}^n w_i \mathbb{1}\{\mathbf{X}_{(i)} \leq \mathbf{x}, Y_{(i)} \leq t\}$ be the corresponding empirical measure.

Then, there exists a constant C depending on M_3 such that

$$\mathbb{E}W(\hat{F}_{\mathbf{X},T}, F_{\mathbf{X},T}) \leq Cn^{-\frac{1}{p+1}}. \quad (14)$$

Proposition 1 is developed based on Proposition 3.1 in Lu and Lu (2020), which is for data without censoring. Comparable to the result in Lu and Lu (2020), (14) indicates that the rate, at which the Kaplan-Meier estimator converges to the truth in distribution, is the same as the empirical distribution estimator. Finally, with Proposition 1, Theorem 1 and Theorem 2 hold for the weighted penalized WGAN for survival data analysis.

5 Simulation

We conduct simulation to gauge performance of the proposed approach. For comparison, we consider the following highly relevant alternatives using neural networks: least squares with group Lasso penalization (P-LS, Yuan and Lin, 2006), deep feature selection with a selection layer (DFS, Chen et al., 2021), LassoNet (Lemhadri et al., 2021), and the group concave regularization method (GCRNet, Luo and Halabi, 2023). Specifically, with P-LS, neural network is adopted for nonparametric estimation, and the group Lasso penalization is applied to the first-layer weights. GCRNet applies the minimax concave penalty (MCP) to the first layer-weights for feature selection. Both DFS and LassoNet have special network architectures. In particular, DFS adds an one-to-one selection layer to the

network. LassoNet adds a single residual layer to the network, connecting predictors and response, and selection is achieved by allowing a feature to participate in any hidden layer only if its residual-layer representative is active. Among the alternatives, P-LS can be applied to survival data by changing the least squares objective function to the weighted form corresponding to the AFT model. LassoNet and GCRNet can be applied to survival data by building on the Cox regression. DFS cannot be directly applied to survival data. We acknowledge that the field is moving fast and there are other applicable alternatives. The above ones are arguably more popular, have competitive performance, and have been adopted in multiple studies. We implement the proposed method in Pytorch and use the stochastic gradient descent algorithm RMSprop in the training process. For the alternatives, computation follows the original developments. We simulate data from the following models:

M 1. *A linear model with an additive standard normal error: $Y = \mathbf{X}^\top \boldsymbol{\beta} + \epsilon$, where $\boldsymbol{\beta} = (\mathbf{1}_{30}^\top, \mathbf{0}_{pc}^\top)^\top$ and $\epsilon \sim N(0, 1)$.*

M 2. *A linear model with an additive heavy-tail error: $Y = \mathbf{X}^\top \boldsymbol{\beta} + \epsilon$, where $\boldsymbol{\beta} = (\mathbf{1}_{30}^\top, \mathbf{0}_{pc}^\top)^\top$ and $\epsilon \sim t(1)$.*

M 3. *A nonlinear model with an additive standard normal error: $Y = \mathbf{X}^\top \boldsymbol{\beta} + \exp(X_2 + \frac{1}{3}X_3) + \sin(X_4X_5)\epsilon$, where $\boldsymbol{\beta} = (\mathbf{1}_{30}^\top, \mathbf{0}_{pc}^\top)^\top$ and $\epsilon \sim N(0, 1)$.*

M 4. *A nonlinear model in the form of a fully connected network with a product standard normal error: $Y = (\mathbf{w}_1 \sigma(\mathbf{w}_0 \mathbf{X} + \mathbf{b}_0) + b_1)\epsilon$, where function σ is component-wise defined as $\sigma(X) = \max(0.01X, X)$, $\mathbf{w}_0 \in \mathbb{R}^{16 \times d}$ is a fixed matrix with the first 30 columns non-zero, $\mathbf{w}_1 \in \mathbb{R}^{16}$, $\mathbf{b}_0 \in \mathbb{R}^{16}$ and $b_1 \in \mathbb{R}$ are fixed vectors – specifically, they are generated from a standard normal distribution and then kept fixed, and $\epsilon \sim N(0, 1)$.*

M 5. A nonlinear AFT (accelerated failure time) model with a predictor-dependent censoring mechanism: $T = |\mathbf{X}^\top \boldsymbol{\beta}(1 - \mathbf{X}^\top \boldsymbol{\beta})|^{1/2} + |\mathbf{X}^\top \boldsymbol{\beta}| |\epsilon|$, where $C = 4 \exp(\mathbf{X}^\top \boldsymbol{\beta})$, $\epsilon \sim N(0, 1)$, and $\boldsymbol{\beta} = (\mathbf{1}_{30}^\top, \mathbf{0}_{p_c}^\top)^\top$.

M 6. A nonlinear AFT model with a predictor-dependent censoring mechanism:

$$T = \begin{cases} \exp(\sqrt{0.1|\mathbf{X}^\top \boldsymbol{\beta}|}) - 1.1 + 0.3|\epsilon| & 2\mathbf{X}^\top \boldsymbol{\beta} \in (-\infty, -6.5] \\ |0.7X_1^3 + 0.2X_2^2 + 0.3X_3 + \epsilon| & 2\mathbf{X}^\top \boldsymbol{\beta} \in (-6.5, 0] \\ \exp(0.4\mathbf{X}^\top \boldsymbol{\beta} + \epsilon) & 2\mathbf{X}^\top \boldsymbol{\beta} \in (0, 6.5] \\ |\log(3\mathbf{X}^\top \boldsymbol{\beta} + \epsilon)| & 2\mathbf{X}^\top \boldsymbol{\beta} \in (6.5, \infty) \end{cases},$$

where $C = 4 \exp(\mathbf{X}^\top \boldsymbol{\beta})$, $\epsilon \sim N(0, 1)$, and $\boldsymbol{\beta} = (\mathbf{1}_{30}^\top, \mathbf{0}_{p_c}^\top)^\top$.

For all the models, the predictors are generated from a multivariate standard normal distribution with dimension $p \in \{100, 300, 500, 1000\}$. The censoring rates for M5 and M6 are about 45% and 40%, respectively. Both the generator network and discriminator network have two hidden layers with widths (64, 32). The noise vector $\mathbf{Z} \sim N(\mathbf{0}, \mathbf{I}_5)$. For the training datasets, we generate 1,000 samples for M1 and M3, 10,000 samples for M2 and M4, and 5,000 samples for M5 and M6. The differences in sample size have been motivated by the differences in model complexity. The sizes of the validation datasets (which are used for network parameter tuning) and testing datasets (which are used for prediction performance evaluation) are 100 and 1,000, respectively. For each model, we simulate 100 replicates.

Variable selection performance is evaluated using true positive rate (TPR) and false positive rate (FPR) which are defined as: $\text{TPR} = \frac{|\hat{S} \cap S^*|}{|S^*|}$, and $\text{FPR} = \frac{|\hat{S} \cap S^c|}{|S^c|}$, where $|\cdot|$ is the cardinality of a set, \hat{S} , S^* , and S^c are the sets of the empirically selected variables, the important variables, and the unimportant variables, respectively. Prediction is evaluated

Table 1: Simulation results for variable selection and prediction with $p_s = 30$.

p	Proposed			P-LS			DFS			LassoNet			GCRNet			
	MSE/C-idx	TPR	FPR													
M1	100	1.50(0.06)	1.00	0.00	1.13(0.05)	1.00	0.00	1.61(0.47)	0.99	0.00	1.08(0.04)	1.00	0.00	1.59(0.09)	1.00	0.11
	300	1.51(0.13)	1.00	0.00	1.23(0.12)	1.00	0.00	1.71(0.52)	0.98	0.00	1.13(0.06)	1.00	0.00	1.62(0.10)	1.00	0.05
	500	1.54(0.24)	1.00	0.00	1.35(0.08)	1.00	0.00	1.85(0.55)	0.98	0.00	1.17(0.04)	1.00	0.00	1.66(0.08)	1.00	0.03
	1000	1.57(0.16)	1.00	0.00	1.42(0.17)	1.00	0.00	1.98(0.57)	0.97	0.00	1.18(0.05)	1.00	0.00	1.68(0.09)	1.00	0.01
M2	100	-	1.00	0.00	-	0.58	0.46	-	0.36	0.27	-	1.00	0.32	-	0.06	0.05
	300	-	0.98	0.03	-	0.49	0.48	-	0.18	0.09	-	1.00	0.12	-	0.09	0.08
	500	-	0.96	0.01	-	0.45	0.50	-	0.13	0.01	-	1.00	0.19	-	0.00	0.00
	1000	-	0.95	0.02	-	0.60	0.48	-	0.04	0.03	-	1.00	0.25	-	0.00	0.00
M3	100	1.46(0.27)	1.00	0.00	0.61(0.28)	1.00	0.00	1.55(0.22)	1.00	0.00	1.07(0.49)	1.00	0.00	1.67(0.36)	1.00	0.07
	300	1.44(0.27)	1.00	0.00	1.11(0.80)	1.00	0.00	1.55(0.27)	0.98	0.00	1.25(0.65)	1.00	0.00	1.76(0.45)	1.00	0.03
	500	1.45(0.32)	1.00	0.00	1.32(0.69)	1.00	0.00	1.72(0.48)	0.97	0.00	1.29(0.53)	1.00	0.00	1.99(0.64)	1.00	0.01
	1000	1.49(0.36)	1.00	0.00	1.45(0.49)	1.00	0.00	1.96(0.46)	0.97	0.00	1.66(0.40)	1.00	0.00	2.10(0.67)	1.00	0.00
M4	100	8.69(1.03)	1.00	0.00	8.53(1.04)	0.47	0.48	8.97(0.91)	0.28	0.31	8.51(0.87)	1.00	0.84	8.47(1.02)	0.00	0.00
	300	8.66(0.93)	1.00	0.00	7.55(0.67)	0.52	0.51	8.95(0.83)	0.13	0.10	8.71(0.89)	1.00	1.00	8.53(0.81)	0.00	0.00
	500	7.72(0.73)	0.98	0.00	9.21(0.81)	0.48	0.43	8.82(0.93)	0.07	0.06	8.57(0.86)	1.00	1.00	8.94(0.92)	0.00	0.00
	1000	8.01(0.76)	0.99	0.00	9.65(0.97)	0.52	0.50	8.17(0.66)	0.05	0.03	9.72(0.84)	1.00	1.00	9.13(0.72)	0.00	0.00
M5	100	0.90(0.01)	1.00	0.00	0.91(0.01)	1.00	0.00	-	-	-	0.83(0.01)	0.95	0.00	0.79(0.01)	1.00	0.66
	300	0.91(0.01)	1.00	0.00	0.91(0.01)	1.00	0.00	-	-	-	0.82(0.01)	0.97	0.01	0.79(0.01)	1.00	0.52
	500	0.91(0.01)	1.00	0.00	0.91(0.01)	1.00	0.00	-	-	-	0.82(0.01)	0.96	0.00	0.79(0.01)	1.00	0.35
	1000	0.91(0.01)	1.00	0.00	0.91(0.01)	1.00	0.00	-	-	-	0.80(0.02)	1.00	0.63	0.79(0.01)	1.00	0.17
M6	100	0.83(0.01)	0.99	0.00	0.79(0.02)	0.85	0.00	-	-	-	0.71(0.01)	0.63	0.08	0.49(0.01)	0.00	0.00
	300	0.83(0.01)	0.99	0.00	0.78(0.02)	0.81	0.06	-	-	-	0.68(0.01)	0.54	0.01	0.50(0.00)	0.00	0.00
	500	0.82(0.01)	0.99	0.00	0.78(0.02)	0.77	0.09	-	-	-	0.67(0.01)	0.44	0.27	0.50(0.01)	0.00	0.00
	1000	0.82(0.01)	0.99	0.00	0.77(0.01)	0.73	0.01	-	-	-	0.67(0.01)	0.45	0.48	0.50(0.00)	0.00	0.00

Note: The standard errors are given in parentheses. With DFS, the number of variables to be selected is set as 30, which is required during the training process.

using the mean square error between the predicted and observed responses on the testing data, denoted by MSE. For continuous response, for example for the proposed approach, it is computed as $T^{-1} \sum_{i=1}^T \|Y_i - J^{-1} \sum_{j=1}^J g_{\hat{\theta}_2}(\mathbf{X}_i, \mathbf{Z}_j)\|_2^2$, where $g_{\hat{\theta}_2}$ is the generator network function trained in the second stage, T is the size of the testing data, and J is the size of the noise samples \mathbf{z} . For survival response, prediction is evaluated using the Concordance index (C-idx) computed as: $\text{C-idx} = \frac{\sum_{i \neq j} \Delta_i \mathbb{1}(\hat{Y}_i \leq \hat{Y}_j) \{1 - 2\mathbb{1}(Y_i \leq Y_j)\}}{\sum_{i \neq j} \Delta_i \mathbb{1}(Y_i \leq Y_j)}$, where \hat{Y}_i is the predicted survival time calculated as $\hat{Y}_i = J^{-1} \sum_{j=1}^J g_{\hat{\theta}_2}(\mathbf{X}_i, \mathbf{Z}_j)$ with $J = 50$.

The variable selection and prediction results are summarized in Table 1. It is observed that the proposed approach has satisfactory variable selection performance with high TPR and low FPR values, while the alternatives fail with Models M2, M4, and M6. In particular, for Model M6 which is especially complicated, the proposed approach is the only one that can satisfactorily identify the important variables under all dimensions of \mathbf{X} . In terms of prediction, it has smaller MSEs than DFS and GCRNet, but may have slightly larger values than P-LS and LassoNet in some cases. This observation aligns with expectation, as the objective functions of the latter methods primarily aim at minimizing mean squared

error, whereas the proposed emphasizes distribution matching. The differences diminish as the dimension of \mathbf{X} increases, suggesting that the proposed approach is less affected by dimensionality. This can be attributed to the proposed two-stage strategy. It is noted that MSE for M2 is not reported because the mean of $t(1)$ is not well defined. Additional numerical results are provided in Appendix, including the evaluation of the distribution estimation and the results with $\mathbf{X}^s \in \mathbb{R}^5$.

6 Data Analysis

To demonstrate practical utility, we analyze three datasets, namely The Cancer Genome Atlas Lung Adenocarcinoma (TCGA-LUAD) data, the Medical Information Mart for Intensive Care III (MIMIC-III) data (Johnson et al., 2016), and the HIV-1 data (Rhee et al., 2006). In the TCGA-LUAD data, both the predictors and response are continuous. In the MIMIC-III data, we conduct two analyses: the first is to identify important biomarkers for albumin level, where both the predictors and response are continuous, and the second is to identify important biomarkers for survival (which is subject to right censoring). In the HIV-1 data, the predictors are binary, and the response is continuous. For the proposed and alternative methods, the implementation details are summarized in Section XX in Appendix.

6.1 TCGA-LUAD data

TCGA is an authoritative cancer omics database. LUAD is a major subtype of lung cancer. This dataset contains 460 samples. For the response variable, we first extract 226 features of tumor pathological images, which describe tumors' micro properties and microenvironment. We then conduct principal component analysis (PCA) and extract the first PC, which can

Table 2: Data analysis: Prediction performance.

	Proposed	P-LS	DFS	LassoNet	GCRNet
TCGA	0.917(0.355)	1.061(0.354)	1.513(0.090)	1.516(0.102)	2.278(0.538)
MIMIC-III (Albumin)	0.082(0.018)	0.104(0.020)	0.084(0.020)	0.363(0.058)	0.378(0.054)
MIMIC-III (Survival)	0.646(0.014)	0.646(0.022)	-	0.630(0.029)	0.563(0.013)
HIV-1 (APV)	0.462(0.049)	0.503(0.055)	0.430(0.042)	0.484(0.049)	0.529(0.063)
HIV-1 (SQV)	0.667(0.059)	0.662(0.056)	0.674(0.064)	0.676(0.053)	0.731(0.066)

Note: Standard errors are given in parentheses. For MIMIC-III (survival data), c-idx is computed instead of MSE. DFS is not applicable to survival data.

describe the most important pathological properties. For predictors, we consider 21,080 gene expressions and apply marginal screening to reduce the dimension to 900. Overall, this analysis examines how tumor properties are affected by gene expressions.

Nine genes are identified by the proposed approach, which are *ST6GAL1*, *ISL2*, *OR10G8*, *WDR89*, *OR4N5*, *TRIM16L*, *C1orf126*, *TMEM159*, *PIK3C2A*. Data is also analyzed using the alternatives considered in simulation. It is observed that different methods lead to different selection results. Out of the four compared methods, P-LS and LassoNet have an overlap in their selection of important genes with the proposed approach. More details are available in Table A.7 in Appendix. To evaluate the stability of selection, we resort to a random sampling-based approach with 30 replications. In each replication, we randomly pick 360 samples for selection/estimation and the rest 100 samples for testing. For the proposed approach, P-LS, and LassoNet, several genes are frequently identified, while DFS selects highly different genes, across the replications. GCRNet identifies zero important genes in 27 replications. The details of the selected genes with their frequencies are given in Table A.8 in Appendix. Additionally, we also evaluate prediction performance. With the estimation results (using the 360 samples), prediction performance is evaluated for the 100 testing samples using MSE. The results are summarized in Table 2. It is observed that the proposed approach has the best prediction performance.

6.2 MIMIC-III data on albumin level

MIMIC-III dataset is a large openly available electronic health records database, comprising rich information related to patients admitted to critical care units between 2001 and 2012. It contains data on 38,597 distinct adult patients and covers 12,587 charted observations in total. We refer to the literature (Deng et al., 2023) for information on data processing. For response, we consider albumin level, which is associated with many diseases such as liver cirrhosis. For predictors, we consider basic information of patients such as gender as well as the charted observations. For each charted observation, the mean and max values are considered (as longitudinal observations are available). The total dimensionality is 155. Those samples with missing response and predictors with missing rates exceeding 40% are excluded from analysis. The remaining missing values are imputed using the sample means. After this processing, the sample size is 2,233.

The proposed approach identifies seven important variables, including one on basic patient information (number of admissions) and six charted observations. Among the charted observations, three pertain to different aspects of white blood cells, which are closely related to albumin level (Tate et al., 2019). Among the remaining three, two represent the mean and max values of Platelets, and the third one is Differential-lymphs. In certain situations such as the diagnosis of liver and kidney diseases, Platelets and Differential-lymphs are considered in conjunction with albumin level (Jørgensen and Stoffersen, 1980). Among the seven identified variables by the proposed approach, DFS identifies five, P-LS identifies four, and LassoNet and GCRNet identify two. More details are provided in Table A.9 in Appendix. The same evaluations as for the TCGA data are conducted. The splitted sets have sizes 1,933 and 300, respectively. The same four variables are consistently identified by the proposed approach across replications, suggesting a high level of stability. The fre-

quently identified variables of each method are given in Table A.10 in Appendix. Table 2 shows that the prediction errors of the proposed approach and DFS are comparable. Additionally, the proposed approach exhibits a prediction error smaller than that of P-LS and significantly smaller than those of LassoNet and GCRNet.

6.3 MIMIC-III data on survival

The same data processing as above is conducted. The analyzed dataset contains 8,323 patients, and the survival times of 5,517 patients are censored. There are a total of 379 predictors, which describe the basic information of the patients as well as the min, mean, and max values of the charted observations. The proposed approach identifies 11 variables, and LassoNet identifies 15 variables. All of those variables are the charted observations. P-LS identifies 14 variables, among which one is on the patients' basic information. GCRNet does not identify any variable. Additional results are provided in Table A.11 in Appendix. In the evaluations, the two splitted sets have sizes 5,323 and 3,000, respectively. Table 2 shows that the c-idx values of the proposed approach and P-LS are the same and slightly larger than LassoNet. For GCRNet, as no significant variable is identified, we use all the variables to compute c-idx, which is much worse than the others.

6.4 HIV-1 drug resistance data

This dataset contains information on 16 drugs from three classes. We specifically consider two drugs that belong to the protease inhibitors class to identify mutations that are associated with them. The response variable is the log-transformed drug resistance level. Each component of the predictor vector \mathbf{X} is a binary variable, representing the presence or absence of a mutation. The samples with missing drug resistance information and the mutations that appear less than three times are removed from analysis. The dimension of

\mathbf{X} is 205. There are 768 samples for Amprenavir (APV) and 826 samples for Saquinavir (SQV).

For both APV and SQV, the proposed approach identifies 24 mutations. P-LS and DFS identify 25 mutations. LassoNet identifies 23 mutations for APV and 25 mutations for SQV. GCRNet identifies 18 mutations for APV and 31 mutations for SQV. The detailed list of the identified mutations can be found in Table A.12 in Appendix. To evaluate identification accuracy, we compare against the expert panel given in Rhee et al. (2006). It can be seen from Table A.13 that the proposed approach identifies a larger number of truly important mutations while having the lowest false discoveries in most cases. The prediction results given in Table 2 show that the prediction error of the proposed approach is comparable to or slightly smaller than most of the others.

References

- Bauer, B. and Kohler, M. (2019). On deep learning as a remedy for the curse of dimensionality in nonparametric regression. *The Annals of Statistics*, 47(4):2261 – 2285.
- Bolte, J., Daniilidis, A., Ley, O., and Mazet, L. (2010). Characterizations of Łojasiewicz inequalities: subgradient flows, talweg, convexity. *Transactions of the American Mathematical Society*, 362(6):3319–3363.
- Chen, Y., Gao, Q., Liang, F., and Wang, X. (2021). Nonlinear variable selection via deep neural networks. *Journal of Computational and Graphical Statistics*, 30(2):484–492.
- Deng, S., Ning, Y., Zhao, J., and Zhang, H. (2023). Optimal and safe estimation for high-dimensional semi-supervised learning. *Journal of the American Statistical Association*, 0(0):1–12.

- Dinh, V. C. and Ho, L. S. (2020). Consistent feature selection for analytic deep neural networks. *Advances in Neural Information Processing Systems*, 33:2420–2431.
- Farrell, M. H., Liang, T., and Misra, S. (2021). Deep neural networks for estimation and inference. *Econometrica*, 89(1):181–213.
- Feng, J. and Simon, N. (2017). Sparse-input neural networks for high-dimensional non-parametric regression and classification. *arXiv preprint arXiv:1711.07592*.
- Gulrajani, I., Ahmed, F., Arjovsky, M., Dumoulin, V., and Courville, A. C. (2017). Improved training of wasserstein gans. *Advances in neural information processing systems*, 30.
- He, X., Wang, J., and Lv, S. (2018). Gradient-induced model-free variable selection with composite quantile regression. *Statistica Sinica*, 28(3):1521–1538.
- Huang, J., Horowitz, J. L., and Wei, F. (2010). Variable selection in nonparametric additive models. *The Annals of Statistics*, 38(4):2282–2313.
- Jiao, Y., Shen, G., Lin, Y., and Huang, J. (2023). Deep nonparametric regression on approximate manifolds: Nonasymptotic error bounds with polynomial prefactors. *The Annals of Statistics*, 51(2):691 – 716.
- Johnson, A. E., Pollard, T. J., Shen, L., Lehman, L.-w. H., Feng, M., Ghassemi, M., Moody, B., Szolovits, P., Anthony Celi, L., and Mark, R. G. (2016). Mimic-iii, a freely accessible critical care database. *Scientific data*, 3(1):1–9.
- Jørgensen, K. A. and Stoffersen, E. (1980). On the inhibitory effect of albumin on platelet aggregation. *Thrombosis research*, 17(1):13–18.
- Kallenberg, O. (2002). *Foundations of Modern Probability*. Springer.

- Lei, J. (2020). Convergence and concentration of empirical measures under Wasserstein distance in unbounded functional spaces. *Bernoulli*, 26(1):767 – 798.
- Lemhadri, I., Ruan, F., Abraham, L., and Tibshirani, R. (2021). Lassonet: A neural network with feature sparsity. *The Journal of Machine Learning Research*, 22(1):5633–5661.
- Li, B., Tang, S., and Yu, H. (2019). Better approximations of high dimensional smooth functions by deep neural networks with rectified power units. *Communications in Computational Physics*.
- Li, B., Tang, S., and Yu, H. (2020). Powernet: Efficient representations of polynomials and smooth functions by deep neural networks with rectified power units. *Journal of Mathematical Study*, 53(2):159–191.
- Li, Y., Chen, C.-Y., and Wasserman, W. W. (2016). Deep feature selection: theory and application to identify enhancers and promoters. *Journal of Computational Biology*, 23(5):322–336.
- Liang, F., Li, Q., and Zhou, L. (2018). Bayesian neural networks for selection of drug sensitive genes. *Journal of the American Statistical Association*, 113(523):955–972.
- Liu, H., Wasserman, L., Lafferty, J., and Ravikumar, P. (2007). Spam: Sparse additive models. In *Advances in Neural Information Processing Systems*, volume 20.
- Liu, S., Zhou, X., Jiao, Y., and Huang, J. (2021). Wasserstein generative learning of conditional distribution. *arXiv*, 2112.10039.
- Lu, Y., Fan, Y., Lv, J., and Stafford Noble, W. (2018). Deeppink: reproducible feature

- selection in deep neural networks. *Advances in neural information processing systems*, 31.
- Lu, Y. and Lu, J. (2020). A universal approximation theorem of deep neural networks for expressing probability distributions. volume 33, pages 3094–3105.
- Luo, B. and Halabi, S. (2023). Sparse-input neural network using group concave regularization. *arXiv preprint arXiv:2307.00344*.
- Padilla, O. H. M., Tansey, W., and Chen, Y. (2020). Quantile regression with relu networks: Estimators and minimax rates. *Journal of Machine Learning Research*, 23:247:1–247:42.
- Pham, T. S. (2012). An explicit bound for the Łojasiewicz exponent of real polynomials. *Kodai Mathematical Journal*, 35(2):311 – 319.
- Rhee, S.-Y., Taylor, J., Wadhwa, G., Ben-Hur, A., Brutlag, D. L., and Shafer, R. W. (2006). Genotypic predictors of human immunodeficiency virus type 1 drug resistance. *Proceedings of the National Academy of Sciences*, 103(46):17355–17360.
- Scardapane, S., Comminiello, D., Hussain, A., and Uncini, A. (2017). Group sparse regularization for deep neural networks. *Neurocomputing*, 241:81–89.
- Schmidt-Hieber, J. (2020). Nonparametric regression using deep neural networks with relu activation function. *Annals of statistics*, 48:1875–1897.
- Shen, G., Jiao, Y., Lin, Y., Horowitz, J. L., and Huang, J. (2022). Estimation of non-crossing quantile regression process with deep relu neural networks. *arXiv preprint arXiv:2207.10442*.
- Shen, G., Jiao, Y., Lin, Y., and Huang, J. (2021). Robust nonparametric regression with deep neural networks. *arXiv preprint arXiv:2107.10343*.

- Stute, W. (1996). Distributional convergence under random censorship when covariables are present. *Scandinavian Journal of Statistics*, 23(4):461–471.
- Sun, Y., Song, Q., and Liang, F. (2022). Consistent sparse deep learning: Theory and computation. *Journal of the American Statistical Association*, 117(540):1981–1995.
- Tate, J. P., Sterne, J. A., Justice, A. C., Study, V. A. C., (ART-CC, A. T. C. C., et al. (2019). Albumin, white blood cell count, and body mass index improve discrimination of mortality in hiv-positive individuals. *AIDS (London, England)*, 33(5):903.
- Van Der Vaart, A. W., Wellner, J. A., van der Vaart, A. W., and Wellner, J. A. (1996). *Weak convergence*. Springer.
- Villani, C. (2009). *Optimal Transport: Old and New*. Springer.
- Yang, Y., Li, Z., and Wang, Y. (2022). On the capacity of deep generative networks for approximating distributions. *Neural Networks*, 145:144–154.
- Yuan, M. and Lin, Y. (2006). Model selection and estimation in regression with grouped variables. *Journal of the Royal Statistical Society Series B: Statistical Methodology*, 68(1):49–67.
- Zhang, C.-H. (2010). Nearly unbiased variable selection under minimax concave penalty. *The Annals of Statistics*, 38(2):894 – 942.
- Zhao, L., Hu, Q., and Wang, W. (2015). Heterogeneous feature selection with multi-modal deep neural networks and sparse group lasso. *IEEE Transactions on Multimedia*, 17(11):1936–1948.
- Zou, H. and Hastie, T. (2005). Regularization and variable selection via the elastic net. *Journal of the royal statistical society: series B (statistical methodology)*, 67(2):301–320.

Appendix

A.1 Conditions

Denote the class of FNNs with input dimension p_0 , width \mathcal{W} , and depth \mathcal{L} by $\mathcal{NN}(p_0, \mathcal{W}, \mathcal{L})$.

Let \mathbb{N}_0 and \mathbb{N}^+ be the set of non-negative integers and of positive integers, respectively.

For a positive constant c , $\lfloor c \rfloor$ denotes the largest integer strictly smaller than c .

A.1.1 Assumed Conditions

Condition 1. Let $\mathbf{V} = (\mathbf{X}, Y) \sim P_{\mathbf{X}, Y}$. For some $\delta > 0$, \mathbf{V} satisfies the first moment tail condition $\mathbb{E}\|\mathbf{V}\| \mathbb{1}\{\|\mathbf{V}\| > \log t\} = O(t^{-(\log t)^\delta/(p+1)})$, for any $t \geq 1$.

Condition 2. The dimension of important features p_s is fixed, and there exists a constant $c_s > 0$ such that $\min_{1 \leq j \leq p_s} |\mathbb{E}_{\mathbf{X}, Y}[Y|\mathbf{X}^{[j]}(0)] - \mathbb{E}_{\mathbf{X}, Y}[Y|\mathbf{X}]| \geq c_s$, where $\mathbf{X}^{[j]}(0) = (X^{[1]}, \dots, X^{[j-1]}, 0, X^{[j+1]}, \dots, X^{[p]})$.

Condition 3. The function g^* defined in (6) belongs to the Hölder class $\mathcal{H}^\beta(\mathcal{X} \times \mathcal{Z}, B_0)$ for a given $\beta > 0$ and a finite constant $B_0 > 0$, which is defined as

$$\mathcal{H}^\beta(\mathcal{X} \times \mathcal{Z}, B_0) = \left\{ f : \mathcal{X} \times \mathcal{Z} \rightarrow \mathbb{R}, \max_{\|\alpha\|_1 \leq \lfloor \beta \rfloor} \|\partial^\alpha f\|_\infty \leq B_0, \max_{\|\alpha\|_1 = \lfloor \beta \rfloor} \sup_{\mathbf{r} \neq \mathbf{s}} \frac{|\partial^\alpha f(\mathbf{r}) - \partial^\alpha f(\mathbf{s})|}{\|\mathbf{r} - \mathbf{s}\|_2^{\beta - \lfloor \beta \rfloor}} \leq B_0 \right\}$$

where $\partial^\alpha = \partial^{\alpha_1} \dots \partial^{\alpha_{m+p}}$ with $\alpha = (\alpha_1, \dots, \alpha_{m+p})^\top \in \mathbb{N}_0^{m+p}$.

Condition 4. The generator class \mathcal{G}_{θ_1} is a class of FNNs with width $\mathcal{W}_{\mathcal{G}_{\theta_1}}^2 \geq 7(p+m)+1$, depth $\mathcal{L}_{\mathcal{G}_{\theta_1}} \geq 2$, and $\mathcal{W}_{\mathcal{G}_{\theta_1}}^2 \mathcal{L}_{\mathcal{G}_{\theta_1}} = cn_1$ with $12 \leq c \leq 384$. Its parameter $\theta \in [-B_2, B_2]^{\mathcal{S}_\theta}$, where $0 < B_2 < \infty$ is a positive constant and \mathcal{S}_θ is the size of network g_{θ_1} .

Condition 5. The class for network function f_{ϕ_1} is $\mathcal{F}_{\phi_1} \equiv \mathcal{NN}(p+1, \mathcal{W}_{\mathcal{F}_{\phi_1}}, \mathcal{L}_{\mathcal{F}_{\phi_1}})$, whose width $\mathcal{W}_{\mathcal{F}_{\phi_1}} = 152(p+1)^2 3^{p+1} N_{f_1} \lceil \log_2(8N_{f_1}) \rceil$, depth $\mathcal{L}_{\mathcal{F}_{\phi_1}} = 84M_{f_1} \lceil \log_2(8M_{f_1}) \rceil + 2(p+1)$, with $N_{f_1}, M_{f_1} \in \mathbb{N}^+$ and $N_{f_1} M_{f_1} \geq \sqrt{n_1}$.

Condition 6. *There exists a positive constant $a \geq 2$ such that*

$$d(\boldsymbol{\theta}, \Theta)^a \lesssim \{W(P_{\mathbf{X}, g_{\boldsymbol{\theta}_1}}(\mathbf{X}, \mathbf{Z}), P_{\mathbf{X}, Y}) - W(P_{\mathbf{X}, g_{\boldsymbol{\theta}_1^*}}(\mathbf{X}, \mathbf{Z}), P_{\mathbf{X}, Y})\}.$$

Condition 1 is a technical condition for dealing with the case where the support of $P_{\mathbf{X}, Y}$ is an unbounded subset of \mathbb{R}^{p+1} and is commonly satisfied. A popular special case is sub-Gaussian. Condition 2 is a condition on minimal detected signal with respect to Definition 1. Similar definitions have been commonly used in the variable selection literature (Huang et al., 2010; He et al., 2018). Condition 3 is a smoothness condition for the target function g^* in (6), which is commonly required in the approximation theory of neural networks (Schmidt-Hieber, 2020; Shen et al., 2021). Conditions 4-5 describe the size of the network $g_{\boldsymbol{\theta}}$ and f_{ϕ} , respectively. Condition 6 is a technical condition and also has roots in the literature. For a fixed network, this condition holds when the network’s activation function is analytic, and can be demonstrated through Lojasewica’s inequality. Several activation functions satisfy this condition, including the classic ones such as the linear function, tanh function, and sigmoid function, as well as the newly developed ReLU-type activation functions such as GeLU, ELU, and PELU. In general, a can be upper-bounded by some positive constant, such as in a polynomial function class, which has been proved by Bolte et al. (2010) and Pham (2012). This condition is sensible, given the close relationship between the polynomial function class and the network class (Li et al., 2019, 2020; Shen et al., 2022).

A.1.2 Conditions for survival analysis

Let F_T , F_C , and F_Y be the distribution functions of the event time T , the censoring time C , and the observed time Y , respectively. Let τ_T , τ_C , and τ_Y be the endpoints of the support

of T , C , and Y , respectively. Then, $1 - F_Y(y) = (1 - F_T(y))(1 - F_C(y))$, resulting from the independence assumption of T and C . In light of $F_{\mathbf{X},T}$, the joint distribution of (\mathbf{X}, T) , denote

$$\tilde{F}_{\mathbf{X},T}(\mathbf{x}, t) = \begin{cases} F_{\mathbf{X},T}(\mathbf{x}, t), & t < \tau_Y, \\ F_{\mathbf{X},T}(\mathbf{x}, \tau_Y^-) + F_{\mathbf{X},T}(\mathbf{x}, \tau_Y) \mathbb{1}\{\tau_Y \in \Omega\}, & t \geq \tau_Y, \end{cases}$$

with Ω denoting the set of atoms of F_Y . Then, two subdistribution functions are defined as follows:

$$\tilde{F}_{\mathbf{X},Y}^1(\mathbf{x}, y) = P(\mathbf{X} \leq \mathbf{x}, Y \leq y, \Delta = 1), \quad \tilde{F}_Y^0(y) = P(Y \leq y, \Delta = 0).$$

For $j = 1, \dots, p$, let

$$\begin{aligned} \gamma_0(y) &= \exp \left\{ \int_0^{y^-} \frac{\tilde{F}_Y^0(du)}{1 - F_Y(u)} \right\}, \\ \gamma_{1,j}(y) &= \frac{1}{1 - F_Y(y)} \int \mathbb{1}\{y < u\} f(\mathbf{x}, u) \gamma_0(u) \tilde{F}_{\mathbf{X},Y}^1(d\mathbf{x}, dz), \\ \gamma_{2,j}(y) &= \int \int \frac{\mathbb{1}\{\eta < y, \eta < z\} f(\mathbf{x}, z) \gamma_0(z)}{[1 - F_Y(\eta)]^2} \tilde{F}_Y^0(d\eta) \tilde{F}_{\mathbf{X},Y}^1(d\mathbf{x}, dz). \end{aligned}$$

The following conditions are assumed.

Condition 7. T and C are independent and $P(T \leq C|T, \mathbf{X}) = P(T \leq C|\mathbf{X})$.

Condition 8. (X, Y, Δ) satisfies

$$\begin{aligned} \mathbb{E}_{\mathbf{X},T}[f(\mathbf{X}, Y)\gamma_0(Y)\Delta]^2 &< \infty, \\ \int |f(\mathbf{x}, z)|K^{1/2}(u)\tilde{F}_{\mathbf{X},T}(d\mathbf{x}, du) &< \infty, \text{ where } K(y) = \int_0^{y^-} \frac{F_C(du)}{[(1 - F_Y(u))(1 - F_C(u))]} \end{aligned}$$

These two conditions have been commonly assumed.

A.2 Additional Supporting Lemmas

Lemma 1. *Suppose that Conditions 1 and 4 hold. Then, for $g_{\hat{\theta}_1} \in \mathcal{G}_{\theta_1}$ obtained in (2),*

$$\mathbb{E} \sup_{f \in \mathcal{F}_{Lip}^1} \left\{ \mathbb{E}_{\mathbf{X}, \mathbf{Z}} f(\mathbf{X}, g_{\hat{\theta}_1}(\mathbf{X}, \mathbf{Z})) - \frac{1}{n_1} \sum_{i=1}^{n_1} f(\mathbf{X}_i, g_{\hat{\theta}_1}(\mathbf{X}_i, \mathbf{Z}_i)) \right\} \lesssim n_1^{-1/(p+1)} \log n_1, \quad (15)$$

where \mathbb{E} is the expectation taken with respect to $\{(\mathbf{X}_i, Y_i)\}_{i=1}^{n_1}$ and $\{\mathbf{Z}_i\}_{i=1}^{n_1}$.

Proof. The proof will be done in two steps.

Let $\{(\mathbf{X}'_i, Y'_i)\}_{i=1}^{n_1}$ and $\{\mathbf{Z}'_i\}_{i=1}^{n_1}$ be n_1 i.i.d. copies of the random vector (\mathbf{X}, Y) and \mathbf{Z} , respectively. Let $\boldsymbol{\xi} = (\xi_1, \dots, \xi_{n_1})$ be i.i.d. Rademacher variables, i.e., uniform $\{-1, 1\}$.

With the symmetrization technique, we can bound the right hand side of (15) as

$$\begin{aligned} & \mathbb{E} \sup_{f \in \mathcal{F}_{Lip}^1} \left\{ \mathbb{E}_{\mathbf{X}, \mathbf{Z}} f(\mathbf{X}, g_{\hat{\theta}_1}(\mathbf{X}, \mathbf{Z})) - \frac{1}{n_1} \sum_{i=1}^{n_1} f(\mathbf{X}_i, g_{\hat{\theta}_1}(\mathbf{X}_i, \mathbf{Z}_i)) \right\} \\ &= \mathbb{E} \sup_{f \in \mathcal{F}_{Lip}^1} \left\{ \mathbb{E}_{\mathbf{X}', \mathbf{Z}'} \frac{1}{n_1} \sum_{i=1}^{n_1} f(\mathbf{X}'_i, g_{\hat{\theta}_1}(\mathbf{X}'_i, \mathbf{Z}'_i)) - \frac{1}{n_1} \sum_{i=1}^{n_1} f(\mathbf{X}_i, g_{\hat{\theta}_1}(\mathbf{X}_i, \mathbf{Z}_i)) \right\} \\ &\leq \mathbb{E}_{\mathbf{X}, \mathbf{Z}, \mathbf{X}', \mathbf{Z}'} \left[\sup_{f \in \mathcal{F}_{Lip}^1} \frac{1}{n_1} \sum_{i=1}^{n_1} \left\{ f(\mathbf{X}'_i, g_{\hat{\theta}_1}(\mathbf{X}'_i, \mathbf{Z}'_i)) - f(\mathbf{X}_i, g_{\hat{\theta}_1}(\mathbf{X}_i, \mathbf{Z}_i)) \right\} \right] \\ &= \mathbb{E}_{\mathbf{X}, \mathbf{Z}, \mathbf{X}', \mathbf{Z}', \boldsymbol{\xi}} \left[\sup_{f \in \mathcal{F}_{Lip}^1} \frac{1}{n_1} \sum_{i=1}^{n_1} \xi_i \left\{ f(\mathbf{X}'_i, g_{\hat{\theta}_1}(\mathbf{X}'_i, \mathbf{Z}'_i)) - f(\mathbf{X}_i, g_{\hat{\theta}_1}(\mathbf{X}_i, \mathbf{Z}_i)) \right\} \right] \\ &\leq \mathbb{E}_{\mathbf{X}, \mathbf{Z}, \boldsymbol{\xi}} \left\{ \sup_{f \in \mathcal{F}_{Lip}^1} \frac{1}{n_1} \sum_{i=1}^{n_1} \xi_i f(\mathbf{X}_i, g_{\hat{\theta}_1}(\mathbf{X}_i, \mathbf{Z}_i)) \right\} + \mathbb{E}_{\mathbf{X}', \mathbf{Z}', \boldsymbol{\xi}'} \left\{ \sup_{f \in \mathcal{F}_{Lip}^1} \frac{1}{n_1} \sum_{i=1}^{n_1} \xi_i f(\mathbf{X}'_i, g_{\hat{\theta}_1}(\mathbf{X}'_i, \mathbf{Z}'_i)) \right\} \\ &= 2 \mathbb{E}_{\mathbf{X}, \mathbf{Z}} \mathbb{E}_{\boldsymbol{\xi}} \left\{ \sup_{f \in \mathcal{F}_{Lip}^1} \frac{1}{n_1} \sum_{i=1}^{n_1} \xi_i f(\mathbf{X}_i, g_{\hat{\theta}_1}(\mathbf{X}_i, \mathbf{Z}_i)) \right\} \\ &:= 2 \mathbb{E}_{\mathbf{X}, \mathbf{Z}} \mathcal{R}_n(\mathcal{F}_{Lip}^1 | g_{\hat{\theta}_1}), \end{aligned}$$

where $\mathcal{R}_n(\mathcal{F}_{Lip}^1)$ is the conditional Rademacher complexity of \mathcal{F}_{Lip}^1 given $g_{\hat{\theta}_1}$.

To bound $\mathcal{R}_n(\mathcal{F}_{Lip}^1)$, the chaining method is applied. Let $\alpha_0 = B$ and $\alpha_t = 2^{-t}B$ for any $t \in \mathbb{N}^+$. For each t , let \mathcal{C}_t be a α_t cover of \mathcal{F}_{Lip}^1 with respect to $\|\cdot\|_2$ such that, for any

$f \in \mathcal{F}_{\text{Lip}}^1$, there exists a function $\hat{f}_t \in \mathcal{C}_t$ satisfying $\|f - \hat{f}_t\|_2 \leq \alpha_t$. Let $\hat{f}_0 \equiv 0$, and for any $T \in \mathbb{N}^+$, we have the following chaining expression for f :

$$f = f - \hat{f}_T + \sum_{t=1}^T (\hat{f}_t - \hat{f}_{t-1}).$$

Hence, for any $T \in \mathbb{N}^+$, we decompose the Rademacher complexity as

$$\begin{aligned} \mathcal{R}_n(\mathcal{F}_{\text{Lip}}^1 | g_{\hat{\theta}_1}) &\leq \mathbb{E}_{\xi} \sup_{f \in \mathcal{F}_{\text{Lip}}^1} \frac{1}{n_1} \sum_{i=1}^{n_1} \xi_i \left\{ f(\mathbf{X}_i, g_{\hat{\theta}_1}(\mathbf{X}_i, \mathbf{Z}_i)) - \hat{f}_T(\mathbf{X}_i, g_{\hat{\theta}_1}(\mathbf{X}_i, \mathbf{Z}_i)) \right\} \\ &\quad + \mathbb{E}_{\xi} \sup_{f \in \mathcal{F}_{\text{Lip}}^1} \frac{1}{n_1} \sum_{i=1}^{n_1} \xi_i \left[\sum_{t=1}^T \left\{ \hat{f}_t(\mathbf{X}_i, g_{\hat{\theta}_1}(\mathbf{X}_i, \mathbf{Z}_i)) - \hat{f}_{t-1}(\mathbf{X}_i, g_{\hat{\theta}_1}(\mathbf{X}_i, \mathbf{Z}_i)) \right\} \right]. \end{aligned} \quad (16)$$

By Cauchy-Schwarz inequality, the first term in (16) can be bounded by

$$\frac{1}{n_1} \sum_{i=1}^{n_1} \xi_i \left\{ f(\mathbf{X}_i, g_{\hat{\theta}_1}(\mathbf{X}_i, \mathbf{Z}_i)) - \hat{f}_T(\mathbf{X}_i, g_{\hat{\theta}_1}(\mathbf{X}_i, \mathbf{Z}_i)) \right\} \leq \|\xi\|_2 \|f - \hat{f}_T\|_2 \leq \alpha_T.$$

Then, the second term in (16) is the summation of the empirical Rademacher chaos w.r.t. the function classes $\mathcal{C}_t - \mathcal{C}_{t-1} = \{f_t - f_{t-1} : f_t \in \mathcal{C}_t, f_{t-1} \in \mathcal{C}_{t-1}\}$, $t = 1, 2, \dots, T$. By triangle inequality,

$$\|\hat{f}_t - \hat{f}_{t-1}\|_2 \leq \|\hat{f}_t - f\|_2 + \|f - \hat{f}_{t-1}\|_2 \leq \alpha_t + \alpha_{t-1} = 3\alpha_t.$$

Thus, applying Massart's lemma to $\mathcal{C}_t - \mathcal{C}_{t-1}$, $t = 1, 2, \dots, T$, we can obtain

$$\mathbb{E}_{\xi} \sup_{f \in \mathcal{F}_{\text{Lip}}^1} \frac{1}{n_1} \sum_{i=1}^{n_1} \xi_i \left\{ \hat{f}_t(\mathbf{X}_i, g_{\hat{\theta}_1}(\mathbf{X}_i, \mathbf{Z}_i)) - \hat{f}_{t-1}(\mathbf{X}_i, g_{\hat{\theta}_1}(\mathbf{X}_i, \mathbf{Z}_i)) \right\} \leq \frac{3\alpha_t \sqrt{2 \log(|\mathcal{C}_t| |\mathcal{C}_{t-1}|)}}{\sqrt{n_1}}.$$

Therefore, for any $T \in \mathbb{N}^+$,

$$\begin{aligned}
\mathcal{R}_{n_1}(\mathcal{F}_{\text{Lip}}^1 | g_{\hat{\theta}_1}) &\leq \alpha_T + 3 \sum_{t=1}^T \frac{\alpha_t \sqrt{2 \log(|\mathcal{C}_t| |\mathcal{C}_{t-1}|)}}{\sqrt{n_1}} \\
&\leq \alpha_T + 6 \sum_{t=1}^T \frac{\alpha_t \sqrt{\log(|\mathcal{C}_t|)}}{\sqrt{n_1}} \\
&= \alpha_T + 6 \sum_{t=1}^T \frac{(\alpha_t - \alpha_{t-1}) \sqrt{\log(|\mathcal{C}_t|)}}{\sqrt{n_1}} \\
&\leq \alpha_T + 12 \int_{\alpha_{T+1}}^{\alpha_0} \sqrt{\frac{\log N(\delta, \mathcal{F}_{\text{Lip}}^1, \|\cdot\|_2)}{n_1}} d\delta,
\end{aligned}$$

where $N(\delta, \mathcal{F}_{\text{Lip}}^1, \|\cdot\|_2)$ is the covering number of $\mathcal{F}_{\text{Lip}}^1$ under $\|\cdot\|_2$. For any arbitrary small $\delta > 0$, we can choose T such that $\alpha_{T+1} \leq \delta < \alpha_T$. Thus,

$$\begin{aligned}
\mathcal{R}_{n_1}(\mathcal{F}_{\text{Lip}}^1 | g_{\hat{\theta}_1}) &\leq 2\delta + 12 \int_{\delta/2}^B \sqrt{\frac{\log N(\delta, \mathcal{F}_{\text{Lip}}^1, \|\cdot\|_2)}{n_1}} d\delta \\
&\leq \inf_{0 < \delta < B} \left(4\delta + 12 \int_{\delta}^B \sqrt{\frac{\log N(\delta, \mathcal{F}_{\text{Lip}}^1, \|\cdot\|_2)}{n_1}} d\delta \right) \\
&\leq \inf_{0 < \delta < B} \left(4\delta + 12 \int_{\delta}^B \sqrt{\frac{\log N(\delta, \mathcal{F}_{\text{Lip}}^1, \|\cdot\|_{\infty})}{n_1}} d\delta \right).
\end{aligned}$$

To find the upper bound of the covering number, we utilize Theorem 2.7.1 in Van Der Vaart et al. (1996). Under Condition 1, there exists a positive constant C such that

$$\log N(\delta, \mathcal{F}_{\text{Lip}}^1(\mathcal{X} \times \mathcal{Y}), \|\cdot\|_{\infty}) \leq C \left(\frac{\log n_1}{\delta} \right)^{p+1}.$$

Finally, we can establish the upper bound in (15) as

$$\begin{aligned}
\mathbb{E}_{\mathbf{X}, \mathbf{Z}} \mathcal{R}_n(\mathcal{F}_{\text{Lip}}^1 | g_{\hat{\theta}_1}) &\leq 4\delta + \frac{12C}{\sqrt{n_1}} \int_{\delta}^B \left(\frac{\log n_1}{\epsilon} \right)^{\frac{p+1}{2}} d\epsilon \\
&\lesssim \delta + n_1^{-\frac{1}{2}} (\log n_1)^{\frac{p+1}{2}} \delta^{1-\frac{p+1}{2}} \\
&= n_1^{-\frac{1}{p+1}} \log n_1 + n_1^{-\frac{1}{2}} (\log n_1)^{\frac{p+1}{2}} (n_1^{-\frac{1}{p+1}} \log n_1)^{1-\frac{p+1}{2}} \\
&= 2n_1^{-1/(p+1)} \log n_1,
\end{aligned}$$

where the third line holds by taking $\delta = Cn_1^{-\frac{1}{p+1}} \log n_1$. The proof is accomplished. \square

Lemma 2. *Suppose that Condition 1 holds. Then,*

$$\mathbb{E}_{\mathbf{X}_i, Y_i} \sup_{f \in \mathcal{F}_{\text{Lip}}^1} \left\{ \mathbb{E}_{\mathbf{X}, \mathbf{Z}} f(\mathbf{X}, Y) - \frac{1}{n} \sum_{i=1}^n f(\mathbf{X}_i, Y_i) \right\} \lesssim \sqrt{p+1} n^{-1/(p+1)}. \quad (17)$$

Proof. When the third moment of (\mathbf{X}, Y) exists, the result of (17) can be directly obtained from Proposition 3.1 in Lu and Lu (2020). Let $\mathbf{V} = (\mathbf{X}, Y) \sim P_{\mathbf{X}, Y}$. Suppose that Condition 1 holds. By Markov inequality,

$$\Pr(\|\mathbf{V}\| > \log n) \leq \frac{\mathbb{E}\|\mathbf{V}\| \mathbb{1}\{\|\mathbf{V}\| > \log n\}}{\log n} = O\left(n^{-\frac{(\log n)^\delta}{p+1}} / \log n\right).$$

Thus,

$$\mathbb{E}|\mathbf{V}|^3 = \int_0^\infty 3t^2 P(|\mathbf{V}| > t) dt = \int_0^\infty O(1) 3t \exp\left(-\frac{t^{1+\delta}}{d+1}\right) dt < \infty.$$

\square

Lemma 3 (Theorem 2.1 in Yang et al. (2022)). *Suppose that Conditions 1-4 hold. Then,*

$$\min_{g_{\theta_1} \in \mathcal{G}_{\theta_1}} W(P_{\mathbf{X}, g_{\theta_1}}, P_{\mathbf{X}, Y}) \lesssim 2^{1/(p+m)} n_1^{-1/(p+m)}. \quad (18)$$

Lemma 4. *Suppose that Conditions 1-5 hold. Then,*

$$\sup_{f \in \mathcal{F}_{Lip}^1} \inf_{f_{\phi_1} \in \mathcal{F}_{\phi_1}} \|f - f_{\phi_1}\|_{\infty} \leq 76(p+1)^{3/2} n_1^{-1/(p+1)} \log n_1. \quad (19)$$

Remark 2. *Lemmas 3-4 establish the approximation error of the generator network g_{θ_1} and the discriminator network f_{ϕ_1} , respectively. It is noted that they are non-asymptotic. That is, (18) and (20) are valid for arbitrary networks g_{θ_1} and f_{ϕ_1} satisfying Condition 4 and Condition 5, regardless of $n \rightarrow \infty$.*

Proof. The left hand side of (20) is the approximation error of discriminator network f_{ϕ_1} , which gets smaller with network class \mathcal{F}_{ϕ_1} getting larger, intuitively. Refer to Corollary 3.1 in Jiao et al. (2023), if the Lipschitz continuous function f is defined on the bounded support $\mathcal{X} \times \mathcal{Y} = [0, 1]^{p+1}$. Then, for any $N_{f_1}, M_{f_1} \in \mathbb{N}^+$, there exists a function f_{ϕ_1} implemented by a ReLU network with width $\mathcal{W}_{\phi_1} = 152(p+1)^2 3^{p+1} N_{f_1} \lceil \log_2(8N_{f_1}) \rceil$ and depth $\mathcal{L}_{\phi_1} = 84M_{f_1} \lceil \log_2(8M_{f_1}) \rceil + 2(p+1)$ such that

$$\|f - f_{\phi_1}\|_{\infty} \leq 76(p+1)^{3/2} (N_{f_1} M_{f_1})^{-2/(p+1)}.$$

Based on this result, when Condition 1 holds and network class \mathcal{F}_{ϕ_1} satisfies Condition 5,

$$\sup_{f \in \mathcal{F}_{Lip}^1} \inf_{f_{\phi_1} \in \mathcal{F}_{\phi_1}} \|f - f_{\phi_1}\|_{\infty} \leq 76(p+1)^{3/2} (N_{f_1} M_{f_1})^{-2/(p+1)} \log n_1. \quad (20)$$

□

Lemma 5. Under Conditions 1-5, when $p = o(\log n_1)$, for $g_{\theta_1^*} \in \arg \min_{g_{\theta_1} \in \mathcal{G}_{\theta_1}} W(P_{\mathbf{X}, g_{\theta_1}}, P_{\mathbf{X}, Y})$,

(i) its first-layer weights $\mathbf{w}_0(\theta^*) = (\boldsymbol{\mu}^*, \boldsymbol{\nu}^*, \mathbf{v}^*)$ satisfies that $\|\boldsymbol{\mu}^{*[j]}\|_2 \neq 0, \forall j = 1, \dots, p_s$;

(ii) there exists a subset of $g_{\theta_1^*}$, whose first-layer parameters $\mathbf{w}_0(\theta^*) = (\boldsymbol{\mu}^*, \mathbf{0}, \mathbf{v}^*)$.

Remark 3. The proof of (i) is carried out through a contradiction. We first assume that there exists a $\|\boldsymbol{\mu}^{*[j]}\|_2 = 0$ with $j \in \{1, \dots, p_s\}$. Then, the proof is accomplished by showing that the approximation error of $g_{\theta_1^*}$ with such parameters cannot converge to zero, which contradicts Lemma 3. The proof of (ii) follows a constructive approach.

Proof. Recall that the noise-outsourcing lemma guarantees that there exists a measurable function g^* such that $W(P_{\mathbf{X}, g^*}, P_{\mathbf{X}, Y}) = 0$. Hence, by the definition of $g_{\theta_1^*}$ and Lemma 3, under Conditions 1-4,

$$W(P_{\mathbf{X}, g_{\theta_1^*}}, P_{\mathbf{X}, g^*}) = W(P_{\mathbf{X}, g_{\theta_1^*}}, P_{\mathbf{X}, Y}) \lesssim 2^{1/(p+m)} n_1^{-1/(p+m)} \rightarrow 0, \quad (21)$$

when $p = o(\log n_1)$ and $n_1 \rightarrow \infty$. Then, we prove two statements sequentially.

(i). Suppose that there exists a $g_{\theta_1^*}$ whose first-layer weights $\mathbf{w}_0(\theta^*) = (\boldsymbol{\mu}^*, \boldsymbol{\nu}^*, \mathbf{v}^*)$ satisfy $\|\boldsymbol{\mu}^{*[j]}\|_2 = 0$ for at least one $j \in \{1, \dots, p_s\}$. We introduce a random variable V , and for any random vector $\mathbf{X} \in \mathcal{X}$, we construct the vector $\mathbf{X}^{[j]}(0) = (X^{[1]}, \dots, X^{[j-1]}, 0, X^{[j+1]}, \dots, X^{[p]})$, so that $g_{\theta_1^*}(\mathbf{X}^{[j]}(0), \mathbf{Z}) = g_{\theta_1^*}(\mathbf{X}, \mathbf{Z})$. Under Condition 2, for the Wasserstein distance be-

tween $P_{\mathbf{X}, g_{\theta_1^*}}$ and $P_{\mathbf{X}, g^*}$,

$$\begin{aligned}
& W(P_{\mathbf{X}, g_{\theta_1^*}}, P_{\mathbf{X}, g^*}) \\
&= \sup_{f \in \mathcal{F}_{\text{Lip}}^1} \{ \mathbb{E}_{\mathbf{X}, \mathbf{Z}} f(\mathbf{X}, g_{\theta_1^*}(\mathbf{X}, \mathbf{Z})) - \mathbb{E}_{\mathbf{X}, \mathbf{Z}} f(\mathbf{X}, g^*(\mathbf{X}, \mathbf{Z})) \} \\
&\geq \mathbb{E}_{\mathbf{X}, \mathbf{Z}} |\tilde{f}(\mathbf{X}, g_{\theta_1^*}(\mathbf{X}, \mathbf{Z})) - \tilde{f}(\mathbf{X}, g^*(\mathbf{X}, \mathbf{Z}))| \\
&= \mathbb{E}_{\mathbf{X}, \mathbf{Z}} |g_{\theta_1^*}(\mathbf{X}, \mathbf{Z}) - g^*(\mathbf{X}, \mathbf{Z})| \\
&\geq |\mathbb{E}_{\mathbf{X}, \mathbf{Z}} g_{\theta_1^*}(\mathbf{X}^{[j]}(0), \mathbf{Z}) - \mathbb{E}_{\mathbf{X}, \mathbf{Z}} g^*(\mathbf{X}, \mathbf{Z})| \\
&= |\mathbb{E}_{\mathbf{X}, \mathbf{Z}} g_{\theta_1^*}(\mathbf{X}^{[j]}(0), \mathbf{Z}) - \mathbb{E}_{\mathbf{X}, \mathbf{Z}} g^*(\mathbf{X}^{[j]}(0), \mathbf{Z}) + \mathbb{E}_{\mathbf{X}, \mathbf{Z}} g^*(\mathbf{X}^{[j]}(0), \mathbf{Z}) - \mathbb{E}_{\mathbf{X}, \mathbf{Z}} g^*(\mathbf{X}, \mathbf{Z})| \\
&\geq \left| |\mathbb{E}_{\mathbf{X}, \mathbf{Z}} g_{\theta_1^*}(\mathbf{X}^{[j]}(0), \mathbf{Z}) - \mathbb{E}_{\mathbf{X}, \mathbf{Z}} g^*(\mathbf{X}^{[j]}(0), \mathbf{Z})| - |\mathbb{E}_{\mathbf{X}, \mathbf{Z}} g^*(\mathbf{X}^{[j]}(0), \mathbf{Z}) - \mathbb{E}_{\mathbf{X}, \mathbf{Z}} g^*(\mathbf{X}, \mathbf{Z})| \right| \\
&\geq c_s,
\end{aligned}$$

where $\tilde{f}: \mathcal{X} \times \mathcal{Y} \rightarrow \mathbb{R}$ is defined as $\tilde{f}(\mathbf{X}, Y) = \mathbf{X} + Y$, belonging to $\mathcal{F}_{\text{Lip}}^1$. $c_s > 0$ is a positive constant defined in Condition 2. The fifth line holds by Condition 1. It contradicts (21).

Thus, for any $j = 1, \dots, p_s$, $\|\boldsymbol{\mu}^{*[j]}\| \neq 0$.

(ii). Pick any $g_{\theta_1^*}$ with first-layer weights $\mathbf{w}_0(\boldsymbol{\theta}^*) = (\boldsymbol{\mu}^*, \boldsymbol{\nu}^*, \mathbf{v}^*)$, shift $\boldsymbol{\nu}^* = \mathbf{0}$, and denote the shifted function by $\tilde{g}_{\theta_1^*}$. Then, we have

$$\begin{aligned}
W(P_{\mathbf{X}, \tilde{g}_{\theta_1^*}}, P_{\mathbf{X}, g^*}) &= \sup_{f \in \mathcal{F}_{\text{Lip}}^1} \{ \mathbb{E}_{\mathbf{X}, \mathbf{Z}} f(\mathbf{X}, \tilde{g}_{\theta_1^*}(\mathbf{X}, \mathbf{Z})) - \mathbb{E}_{\mathbf{X}, \mathbf{Z}} f(\mathbf{X}, g^*(\mathbf{X}, \mathbf{Z})) \} \\
&\leq \mathbb{E}_{\mathbf{X}, \mathbf{Z}} \|(\mathbf{X}, \tilde{g}_{\theta_1^*}(\mathbf{X}, \mathbf{Z}))^\top - (\mathbf{X}, g^*(\mathbf{X}, \mathbf{Z}))^\top\|_2 \\
&= \mathbb{E}_{\mathbf{X}, \mathbf{Z}} |\tilde{g}_{\theta_1^*}(\mathbf{X}, \mathbf{Z}) - g^*(\mathbf{X}, \mathbf{Z})| \\
&= \mathbb{E}_{\mathbf{X}, \mathbf{Z}} |\tilde{g}_{\theta_1^*}(\mathbf{X}, \mathbf{Z}) - g_{\theta_1^*}((\mathbf{X}^s, \mathbf{0}), \mathbf{Z}) + g_{\theta_1^*}((\mathbf{X}^s, \mathbf{0}), \mathbf{Z}) - g^*(\mathbf{X}, \mathbf{Z})| \\
&\leq \mathbb{E}_{\mathbf{X}, \mathbf{Z}} |\tilde{g}_{\theta_1^*}(\mathbf{X}, \mathbf{Z}) - g_{\theta_1^*}((\mathbf{X}^s, \mathbf{0}), \mathbf{Z})| + \mathbb{E}_{\mathbf{X}, \mathbf{Z}} |g_{\theta_1^*}((\mathbf{X}^s, \mathbf{0}), \mathbf{Z}) - g^*(\mathbf{X}, \mathbf{Z})|,
\end{aligned}$$

where the second line holds as f is a 1-Lipschitz function. The first term in the right hand side equals zero as

$$\begin{aligned} & \mathbb{E}_{\mathbf{X}, \mathbf{Z}} |\tilde{g}_{\theta_1^*}(\mathbf{X}, \mathbf{Z}) - g_{\theta_1^*}((\mathbf{X}^s, \mathbf{0}), \mathbf{Z})| \\ &= \mathbb{E}_{\mathbf{X}, \mathbf{Z}} \left| \mathbf{w}_{\mathcal{L}_{g_{\theta_1}}} \sigma(\dots \mathbf{w}_1 \sigma(\boldsymbol{\mu}^* \mathbf{X}^s + \mathbf{0} \mathbf{X}^c + \mathbf{v}^* \mathbf{Z} + \mathbf{b}_0) + \mathbf{b}_1) + \dots) + \mathbf{b}_{\mathcal{L}_{g_{\theta_1}}} \right. \\ & \quad \left. - \mathbf{w}_{\mathcal{L}_{g_{\theta_1}}} \sigma(\dots \mathbf{w}_1 \sigma(\boldsymbol{\mu}^* \mathbf{X}^s + \mathbf{v}^* \mathbf{0} + \mathbf{v}^* \mathbf{Z} + \mathbf{b}_0) + \mathbf{b}_1) + \dots) + \mathbf{b}_{\mathcal{L}_{g_{\theta_1}}} \right| = 0. \end{aligned}$$

Next, consider the second term. Similarly for $\tilde{f}(\cdot)$,

$$\begin{aligned} & \mathbb{E}_{\mathbf{X}, \mathbf{Z}} |g_{\theta_1^*}((\mathbf{X}^s, \mathbf{0}), \mathbf{Z}) - g^*(\mathbf{X}, \mathbf{Z})| \\ &= \mathbb{E}_{\mathbf{X}, \mathbf{Z}} |g_{\theta_1^*}((\mathbf{X}^s, \mathbf{X}^c), \mathbf{Z}) - g^*((\mathbf{X}^s, \mathbf{X}^c), \mathbf{Z}) | \mathbf{X}^c = \mathbf{0}| \\ &\leq \mathbb{E}_{\mathbf{X}, \mathbf{Z}} |g_{\theta_1^*}(\mathbf{X}, \mathbf{Z}) - g^*(\mathbf{X}, \mathbf{Z})| \\ &= \mathbb{E}_{\mathbf{X}, \mathbf{Z}} |\tilde{f}(\mathbf{X}, g_{\theta_1^*}(\mathbf{X}, \mathbf{Z})) - \tilde{f}(\mathbf{X}, g^*(\mathbf{X}, \mathbf{Z}))| \\ &\leq \sup_{f \in \mathcal{F}_{\text{Lip}}^1} \{ \mathbb{E}_{\mathbf{X}, \mathbf{Z}} f(\mathbf{X}, g_{\theta_1^*}(\mathbf{X}, \mathbf{Z})) - \mathbb{E}_{\mathbf{X}, \mathbf{Z}} f(\mathbf{X}, g^*(\mathbf{X}, \mathbf{Z})) \} \\ &= W(P_{\mathbf{X}, g_{\theta_1^*}}, P_{\mathbf{X}, g^*}) \\ &\rightarrow 0, \quad \text{as } n_1 \rightarrow \infty, \end{aligned}$$

where the first line holds because $g^*(\mathbf{X}, \mathbf{Z})$ is trivial to \mathbf{X}^c by Definition 1. \square

Lemma 6. *When Conditions 1-5 hold and $p = o(\log n_1)$, Θ has the following two properties.*

(i) *For all $\boldsymbol{\theta} \in \Theta$ and $j = 1, \dots, p_s$, there exists $c_\mu > 0$ such that $\|\boldsymbol{\mu}^{[j]}\|_2 \geq c_\mu$. (ii) *For any $\boldsymbol{\theta} \in \Theta$, if we set its $\boldsymbol{\nu}$ -components to zero, it still belongs to Θ .**

Proof. Under the same conditions of Lemma 5, for any network function g_{θ_1} with $\boldsymbol{\theta} \in \Theta$,

$$W(P_{\mathbf{X}, g_{\theta_1}}, P_{\mathbf{X}, g^*}) \lesssim (p+1)^{3/2} n_1^{-2/(p+1)} \log n_1 + 2^{1/(p+m)} n_1^{-1/(p+m)},$$

where $g^*(\mathbf{x}, \mathbf{z}) \sim P_{Y|\mathbf{X}=\mathbf{x}}$ for any $\mathbf{x} \in \mathcal{X}$ given by the noise-outsourcing lemma. When $p = o(\log n_1)$ and $n_1 \rightarrow \infty$, the Wasserstein distance $W(P_{\mathbf{X}, g_{\theta_1}}, P_{\mathbf{X}, g^*}) \rightarrow 0$, implying that $g_{\theta_1}(\mathbf{x}, \mathbf{z}) \rightarrow g^*(\mathbf{x}, \mathbf{z}), \forall \mathbf{x} \in \mathcal{X}, \mathbf{z} \in \mathcal{Z}$.

(i) Assume that no such c_μ exists. Thus, there exists $\tilde{\theta}_1 \in \Theta$ such that its first-layer weights $\|\tilde{\boldsymbol{\mu}}^{[j]}\|_2 \rightarrow 0$ as $n_1 \rightarrow \infty$ for a $j \in \{1, \dots, p_s\}$. Since the first p_s components of \mathbf{X} are assumed to be important, for such j , $(\mathbf{x}^{s[-j]}, \mathbf{x}^c) = \mathbf{x}^{[-j]}$. Then, we have

$$|g_{\tilde{\theta}_1}(\mathbf{x}, \mathbf{z}) - g_{\tilde{\theta}_1}(\mathbf{x}^{[-j]}, \mathbf{z})| \rightarrow 0, \forall \mathbf{x} \in \mathcal{X}, \mathbf{z} \in \mathcal{Z}.$$

As $\tilde{\theta}_1 \in \Theta$,

$$g_{\theta_1}(\mathbf{x}, \mathbf{z}) \rightarrow g^*(\mathbf{x}, \mathbf{z}), \text{ and } g_{\theta_1}(\mathbf{x}^{[-j]}, \mathbf{z}) \rightarrow g^*(\mathbf{x}^{[-j]}, \mathbf{z}), \quad \forall \mathbf{x} \in \mathcal{X}, \mathbf{z} \in \mathcal{Z}.$$

Combining the above two expressions leads to the conclusion that

$$g^*(\mathbf{x}, \mathbf{z}) = g^*(\mathbf{x}^{[-j]}, \mathbf{z}),$$

indicating that $P_{Y|\mathbf{X}=\mathbf{x}} \sim P_{Y|\mathbf{X}^{[-j]}=\mathbf{x}^{[-j]}}$. According to Definition 1, it contradicts the fact that $\tilde{\boldsymbol{\mu}}$ connects all the important variables.

(ii) Let $\kappa(\boldsymbol{\theta}_1)$ be the function that set the $\boldsymbol{\nu}$ -component of $\boldsymbol{\theta}$ as a zero matrix. When the conditions of Lemma 5 hold, there exists a $g_{\theta_1^*}$ with first-layer weights $\mathbf{w}_0(\boldsymbol{\theta}^*) = (\boldsymbol{\mu}^*, \mathbf{0}, \mathbf{v}^*)$.

Thus,

$$\begin{aligned} W(P_{\mathbf{X}, g_{\theta_1}}(\mathbf{X}, \mathbf{Z}), P_{\mathbf{X}, Y}) &= W(P_{\mathbf{X}, g_{\theta_1^*}}(\mathbf{X}, \mathbf{Z}), P_{\mathbf{X}, Y}) = W(P_{\mathbf{X}, g_{\theta_1^*}}((\mathbf{X}^s, \mathbf{0}), \mathbf{Z}), P_{\mathbf{X}, Y}) \\ &= W(P_{\mathbf{X}, g_{\theta_1}}((\mathbf{X}^s, \mathbf{0}), \mathbf{Z}), P_{\mathbf{X}, Y}) = W(P_{\mathbf{X}, g_{\kappa(\theta_1)}}(\mathbf{X}, \mathbf{Z}), P_{\mathbf{X}, Y}), \end{aligned}$$

leading to the conclusion that $\kappa(\boldsymbol{\theta}_1) \in \Theta$.

□

A.3 Proof of Theorem 1

The proof is accomplished in four steps.

Step 1. Error analysis of $\mathbb{E}[d(\hat{\boldsymbol{\theta}}_1, \Theta)]$.

First, we construct a generator network $g_{\hat{\boldsymbol{\theta}}_1}$ with parameter $\hat{\boldsymbol{\theta}}_1$ obtained by

$$\hat{\boldsymbol{\theta}}_1 = \arg \min_{\boldsymbol{\vartheta} \in \Theta} \|\hat{\boldsymbol{\theta}}_1 - \boldsymbol{\vartheta}\|_2,$$

such that $\mathbb{E}[d(\hat{\boldsymbol{\theta}}_1, \Theta)] = \|\hat{\boldsymbol{\theta}}_1 - \hat{\boldsymbol{\vartheta}}_1\|_2$.

Under Condition 6, there exists a positive constant a such that

$$\begin{aligned} d(\boldsymbol{\theta}, \Theta)^a &\lesssim \{W(P_{\mathbf{X}, g_{\boldsymbol{\theta}_1}}(\mathbf{X}, \mathbf{Z}), P_{\mathbf{X}, Y}) - W(P_{\mathbf{X}, g_{\boldsymbol{\theta}_1^*}}(\mathbf{X}, \mathbf{Z}), P_{\mathbf{X}, Y})\} \\ &= \{W(P_{\mathbf{X}, g_{\boldsymbol{\theta}_1}}(\mathbf{X}, \mathbf{Z}), P_{\mathbf{X}, Y}) - W(P_{\mathbf{X}, g_{\hat{\boldsymbol{\theta}}_1}}(\mathbf{X}, \mathbf{Z}), P_{\mathbf{X}, Y})\} \\ &= \mathbb{E} \left[\sup_{f \in \mathcal{F}_{\text{Lip}}^1} \left\{ \mathbb{E}_{\mathbf{X}, \mathbf{Z}} f(\mathbf{X}, g_{\boldsymbol{\theta}_1}(\mathbf{X}, \mathbf{Z})) - \mathbb{E}_{\mathbf{X}, Y} f(\mathbf{X}, Y) \right\} \right. \\ &\quad \left. - \sup_{f \in \mathcal{F}_{\text{Lip}}^1} \left\{ \mathbb{E}_{\mathbf{X}, \mathbf{Z}} f(\mathbf{X}, g_{\hat{\boldsymbol{\theta}}_1}(\mathbf{X}, \mathbf{Z})) - \mathbb{E}_{\mathbf{X}, Y} f(\mathbf{X}, Y) \right\} \right], \end{aligned} \tag{22}$$

where $\mathcal{F}_{\text{Lip}}^1 = \{f : \mathbb{R}^{p+1} \rightarrow \mathbb{R}, |f(\mathbf{u}) - f(\mathbf{v})| \leq \|\mathbf{u} - \mathbf{v}\|_2, \mathbf{u}, \mathbf{v} \in \mathbb{R}^{p+1}\}$ is the 1-Lipschitz function class, and the second line holds by the definition of Θ . For the convenience of presentation, we introduce the following notations:

$$\begin{aligned} R(\boldsymbol{\theta}; f) &:= \mathbb{E}_{\mathbf{X}, \mathbf{Z}} f(\mathbf{X}, g_{\boldsymbol{\theta}_1}(\mathbf{X}, \mathbf{Z})) - \mathbb{E}_{\mathbf{X}, Y} f(\mathbf{X}, Y), \\ R_{n_1}(\boldsymbol{\theta}; f) &:= \frac{1}{n_1} \sum_{i=1}^{n_1} f(\mathbf{X}_i, g_{\boldsymbol{\theta}_1}(\mathbf{X}_i, \mathbf{Z}_i)) - \frac{1}{n_1} \sum_{i=1}^{n_1} f(\mathbf{X}_i, Y_i). \end{aligned}$$

Then,

$$\begin{aligned}
d(\boldsymbol{\theta}, \Theta)^a &\lesssim \mathbb{E} \left[\sup_{f \in \mathcal{F}_{\text{Lip}}^1} R(\hat{\boldsymbol{\theta}}_1; f) - \sup_{f \in \mathcal{F}_{\text{Lip}}^1} R(\hat{\boldsymbol{\vartheta}}_1; f) \right] \\
&\leq \mathbb{E} \left[\sup_{f \in \mathcal{F}_{\text{Lip}}^1} \left\{ R(\hat{\boldsymbol{\theta}}_1; f) - R_{n_1}(\hat{\boldsymbol{\theta}}_1; f) \right\} + \sup_{f \in \mathcal{F}_{\text{Lip}}^1} R_{n_1}(\hat{\boldsymbol{\theta}}_1; f) - \sup_{f_{\phi_1} \in \mathcal{F}_{\phi_1}} R_{n_1}(\hat{\boldsymbol{\theta}}_1; f_{\phi_1}) + \sup_{f_{\phi_1} \in \mathcal{F}_{\phi_1}} R_{n_1}(\hat{\boldsymbol{\theta}}_1; f_{\phi_1}) \right. \\
&\quad \left. - \sup_{f_{\phi_1} \in \mathcal{F}_{\phi_1}} R_{n_1}(\hat{\boldsymbol{\vartheta}}_1; f_{\phi_1}) + \sup_{f_{\phi_1} \in \mathcal{F}_{\phi_1}} R_{n_1}(\hat{\boldsymbol{\vartheta}}_1; f_{\phi_1}) - \sup_{f \in \mathcal{F}_{\text{Lip}}^1} R_{n_1}(\hat{\boldsymbol{\vartheta}}_1; f) + \sup_{f \in \mathcal{F}_{\text{Lip}}^1} \left\{ R_{n_1}(\hat{\boldsymbol{\vartheta}}_1; f) - R(\hat{\boldsymbol{\vartheta}}_1; f) \right\} \right] \\
&\leq \mathbb{E} \left[\sup_{f \in \mathcal{F}_{\text{Lip}}^1} \left\{ R(\hat{\boldsymbol{\theta}}_1; f) - R_{n_1}(\hat{\boldsymbol{\theta}}_1; f) \right\} + \sup_{f \in \mathcal{F}_{\text{Lip}}^1} \inf_{f_{\phi_1} \in \mathcal{F}_{\phi_1}} \left\{ R_{n_1}(\hat{\boldsymbol{\theta}}_1; f) - R_{n_1}(\hat{\boldsymbol{\theta}}_1; f_{\phi_1}) \right\} + R_{n_1}(\hat{\boldsymbol{\theta}}_1; \hat{f}_{\phi_1}) \right. \\
&\quad \left. - R_{n_1}(\hat{\boldsymbol{\vartheta}}_1; \hat{f}_{\phi_1}) + \sup_{f_{\phi_1} \in \mathcal{F}_{\phi_1}} \inf_{f \in \mathcal{F}_{\text{Lip}}^1} \left\{ R_{n_1}(\hat{\boldsymbol{\vartheta}}_1; f_{\phi_1}) - R_{n_1}(\hat{\boldsymbol{\vartheta}}_1; f) \right\} + \sup_{f \in \mathcal{F}_{\text{Lip}}^1} \left\{ R_{n_1}(\hat{\boldsymbol{\vartheta}}_1; f) - R(\hat{\boldsymbol{\vartheta}}_1; f) \right\} \right] \\
&\leq 2\mathbb{E} \left[\sup_{f \in \mathcal{F}_{\text{Lip}}^1} \left\{ R(\hat{\boldsymbol{\theta}}_1; f) - R_{n_1}(\hat{\boldsymbol{\theta}}_1; f) \right\} \right] + 2 \sup_{f \in \mathcal{F}_{\text{Lip}}^1} \inf_{f_{\phi_1} \in \mathcal{F}_{\phi_1}} \|f - f_{\phi_1}\|_{\infty} + \mathbb{E} \left[R_{n_1}(\hat{\boldsymbol{\theta}}_1; \hat{f}_{\phi_1}) - R_{n_1}(\hat{\boldsymbol{\vartheta}}_1; \hat{f}_{\phi_1}) \right] \\
&:= \mathcal{E}_1 + \mathcal{E}_2 + \mathcal{E}_3.
\end{aligned}$$

Step 2. Bound the above three errors.

First, \mathcal{E}_1 is the stochastic error, which can be bounded by Lemmas 1 and 2, and \mathcal{E}_2 is the approximation error of the nuisance functional parameter f , whose upper bound is given in (20). Therefore, when Conditions 1 and 5 hold and \mathcal{F}_{ϕ_1} further satisfies that $N_{f_1} M_{f_1} \geq \sqrt{n_1}$, we have

$$\mathbb{E}[d(\hat{\boldsymbol{\theta}}_1, \Theta)^a] \lesssim n_1^{-\frac{1}{p+1}} \log n_1 + (p+1)^{\frac{1}{2}} n_1^{-\frac{1}{p+1}} + (p+1)^{\frac{3}{2}} n_1^{-\frac{2}{p+1}} \log n_1 + \mathcal{E}_3. \quad (23)$$

Next, consider \mathcal{E}_3 . Denote the first-layer weights of $g_{\hat{\boldsymbol{\theta}}_1}$ and $g_{\hat{\boldsymbol{\vartheta}}_1}$ by $\mathbf{w}_0(\hat{\boldsymbol{\theta}}_1) = (\hat{\boldsymbol{\mu}}_{\boldsymbol{\theta}_1}, \hat{\boldsymbol{\nu}}_{\boldsymbol{\theta}_1}, \hat{\boldsymbol{\nu}}_{\boldsymbol{\theta}_1})$ and $\mathbf{w}_0(\hat{\boldsymbol{\vartheta}}_1) = (\hat{\boldsymbol{\mu}}_{\boldsymbol{\vartheta}_1}, \hat{\boldsymbol{\nu}}_{\boldsymbol{\vartheta}_1}, \hat{\boldsymbol{\nu}}_{\boldsymbol{\vartheta}_1})$, respectively. Due to the fact that $(\hat{\boldsymbol{\theta}}_1, \hat{\boldsymbol{\phi}}_1) = \arg \min_{\boldsymbol{\theta}} \max_{\phi_1} l_1(g_{\boldsymbol{\theta}_1}, f_{\phi_1})$,

$$\mathcal{E}_3 = \mathbb{E}[R_{n_1}(\hat{\boldsymbol{\theta}}_1; \hat{f}_{\hat{\phi}_1}) - R_{n_1}(\hat{\boldsymbol{\vartheta}}_1; \hat{f}_{\hat{\phi}_1})] \leq \lambda_n \mathbb{E}[J(\hat{\boldsymbol{\vartheta}}_1) - J(\hat{\boldsymbol{\theta}}_1)], \quad (24)$$

where $J(\boldsymbol{\theta}_1) = \sum_{j=1}^p \|\mathbf{w}_0(\boldsymbol{\theta}_1)^{[j]}\|_2$. Recall the left hand side of (22) $d(\hat{\boldsymbol{\theta}}_1, \Theta)^a = \|\hat{\boldsymbol{\theta}}_1 - \hat{\boldsymbol{\vartheta}}_1\|_2^a$,

where a is a positive constant. We can bound $\lambda_n \mathbb{E}[J(\hat{\boldsymbol{\vartheta}}_1) - J(\hat{\boldsymbol{\theta}}_1)]$ as follows:

$$\begin{aligned}
\lambda_n \mathbb{E}[J(\hat{\boldsymbol{\vartheta}}_1) - J(\hat{\boldsymbol{\theta}}_1)] &= \lambda_n \mathbb{E} \left[\left\{ \sum_{j=1}^{p_s} \|\hat{\boldsymbol{\mu}}_{\hat{\boldsymbol{\vartheta}}_1}^{[j]}\|_2 + \sum_{k=1}^{p_c} \|\hat{\boldsymbol{\nu}}_{\hat{\boldsymbol{\vartheta}}_1}^{[k]}\|_2 \right\} - \left\{ \sum_{j=1}^{p_s} \|\hat{\boldsymbol{\mu}}_{\hat{\boldsymbol{\theta}}_1}^{[j]}\|_2 + \sum_{k=1}^{p_c} \|\hat{\boldsymbol{\nu}}_{\hat{\boldsymbol{\theta}}_1}^{[k]}\|_2 \right\} \right] \\
&\leq \lambda_n \mathbb{E} \left\{ \sum_{j=1}^{p_s} \|\hat{\boldsymbol{\mu}}_{\hat{\boldsymbol{\vartheta}}_1}^{[j]} - \hat{\boldsymbol{\mu}}_{\hat{\boldsymbol{\theta}}_1}^{[j]}\|_2 + \sum_{k=1}^{p_c} \|\hat{\boldsymbol{\nu}}_{\hat{\boldsymbol{\vartheta}}_1}^{[k]} - \hat{\boldsymbol{\nu}}_{\hat{\boldsymbol{\theta}}_1}^{[k]}\|_2 \right\} \\
&\leq \lambda_n \mathbb{E}[\sqrt{p_s} \|\hat{\boldsymbol{\mu}}_{\hat{\boldsymbol{\vartheta}}_1} - \hat{\boldsymbol{\nu}}_{\hat{\boldsymbol{\theta}}_1}\|_2 + \sqrt{p_c} \|\hat{\boldsymbol{\mu}}_{\hat{\boldsymbol{\vartheta}}_1} - \hat{\boldsymbol{\nu}}_{\hat{\boldsymbol{\theta}}_1}\|_2] \\
&\leq \sqrt{2} \lambda_n \mathbb{E}[\sqrt{p} \|\hat{\boldsymbol{\theta}}_1 - \hat{\boldsymbol{\vartheta}}_1\|_2],
\end{aligned}$$

where the first inequality holds by the triangle inequality, and the second inequality holds by Cauchy-Schwarz inequality. Then, as $a > 2$, through Young's inequality

$$\mathbb{E}[\lambda_n \sqrt{p} \|\hat{\boldsymbol{\theta}}_1 - \hat{\boldsymbol{\vartheta}}_1\|_2] \leq \mathbb{E} \left\{ \frac{\|\hat{\boldsymbol{\theta}}_1 - \hat{\boldsymbol{\vartheta}}_1\|_2^a}{a} + \frac{(\lambda_n \sqrt{p})^{a/(a-1)}}{(a-1)/a} \right\}. \quad (25)$$

Finally, combining (23), (24) and (25),

$$\begin{aligned}
\mathbb{E} \|\hat{\boldsymbol{\theta}}_1 - \hat{\boldsymbol{\vartheta}}_1\|_2^a &\lesssim n_1^{-\frac{1}{p+1}} \log n_1 + (p+1)^{\frac{1}{2}} n_1^{-\frac{1}{p+1}} + (p+1)^{\frac{3}{2}} n_1^{-\frac{2}{p+1}} \log n_1 \\
&\quad + \mathbb{E} \left\{ \frac{\|\hat{\boldsymbol{\theta}}_1 - \hat{\boldsymbol{\vartheta}}_1\|_2^a}{a} + \frac{(\lambda_n \sqrt{p})^{a/(a-1)}}{(a-1)/a} \right\},
\end{aligned}$$

leading to the conclusion

$$\begin{aligned}
\mathbb{E}[d(\hat{\boldsymbol{\theta}}_1, \Theta)^a] &\lesssim n_1^{-\frac{1}{p+1}} \log n_1 + (p+1)^{\frac{1}{2}} n_1^{-\frac{1}{p+1}} + (p+1)^{\frac{3}{2}} n_1^{-\frac{2}{p+1}} \log n_1 + (\lambda_n \sqrt{p})^{\frac{a}{a-1}}, \\
&\lesssim n_1^{-\frac{1}{p+1}} \log n_1 + (p+1)^{\frac{3}{2}} n_1^{-\frac{2}{p+1}} \log n_1 + (\lambda_n \sqrt{p})^{\frac{a}{a-1}}.
\end{aligned}$$

The last line holds because the second term is dominated when $p = o(\log n_1)$, as

$$\frac{n_1^{-\frac{1}{p+1}} \log n_1}{n_1^{-\frac{1}{p+1}} (p+1)^{\frac{1}{2}}} = \frac{\log n_1}{(p+1)^{\frac{1}{2}}} = \frac{\log n_1}{(o(\log n_1) + 1)^{1/2}} \rightarrow \infty, \quad \text{as } n_1 \rightarrow \infty.$$

Step 3. Bound $\mathbb{E}\|\hat{\boldsymbol{\nu}}_{\boldsymbol{\theta}_1}\|_2$.

Let $\kappa(\hat{\boldsymbol{\nu}}_1)$ be the function that set the $\boldsymbol{\nu}$ -component of $\boldsymbol{\nu}_1$ as a zero matrix. Because $\hat{\boldsymbol{\nu}}_1 \in \Theta$ and $p = o(\log n_1)$, by Lemma 6, $\kappa(\hat{\boldsymbol{\nu}}_1)$ belongs to Θ as well. Thus,

$$\mathbb{E}[R_{n_1}(\hat{\boldsymbol{\theta}}_1; f_{\hat{\phi}_1}) - R_{n_1}(\kappa(\hat{\boldsymbol{\nu}}_1); f_{\hat{\phi}_1})] \leq \lambda_n \mathbb{E}[J(\kappa(\hat{\boldsymbol{\nu}}_1)) - J(\hat{\boldsymbol{\theta}}_1)].$$

Since $J(\kappa(\hat{\boldsymbol{\nu}}_1)) = \sum_{j=1}^{p_s} \|\hat{\boldsymbol{\mu}}_{\boldsymbol{\nu}_1}^{[j]}\|_2$, following the same error analysis in Step 1, we obtain

$$\begin{aligned} \mathbb{E} \left[\sum_{k=1}^{p_c} \|\hat{\boldsymbol{\nu}}_{\boldsymbol{\theta}_1}^{[k]}\|_2 \right] &\leq \lambda_n^{-1} \mathbb{E}[R_{n_1}(\kappa(\hat{\boldsymbol{\nu}}_1); f_{\hat{\phi}_1}) - R_{n_1}(\hat{\boldsymbol{\theta}}_1; f_{\hat{\phi}_1})] + \mathbb{E} \left[\sum_{j=1}^{p_s} \|\hat{\boldsymbol{\mu}}_{\boldsymbol{\nu}_1}^{[j]}\|_2 - \sum_{j=1}^{p_s} \|\hat{\boldsymbol{\mu}}_{\boldsymbol{\theta}}^{[j]}\|_2 \right] \\ &\lesssim \lambda_n^{-1} \{n_1^{-\frac{1}{p+1}} \log n_1 + (p+1)^{\frac{3}{2}} n_1^{-\frac{2}{p+1}} \log n_1\} + \mathbb{E}[\sqrt{p} \|\hat{\boldsymbol{\theta}}_1 - \boldsymbol{\theta}_1\|_2] \\ &= \lambda_n^{-1} \{n_1^{-\frac{1}{p+1}} \log n_1 + (p+1)^{\frac{3}{2}} n_1^{-\frac{2}{p+1}} \log n_1\} + \sqrt{p} \mathbb{E}[d(\hat{\boldsymbol{\theta}}_1, \Theta)]. \end{aligned}$$

Combining the results of the previous three steps, we reach the conclusion that, under Conditions 1-6, there exists a positive constant $a > 2$ such that

$$\begin{aligned} \mathbb{E}[d(\hat{\boldsymbol{\theta}}_1, \Theta)] &\lesssim \left\{ n_1^{-\frac{1}{p+1}} \log n_1 + (p+1)^{\frac{3}{2}} n_1^{-\frac{2}{p+1}} \log n_1 + (\lambda_n \sqrt{p})^{\frac{a}{a-1}} \right\}^{\frac{1}{a}}, \\ \mathbb{E}\|\hat{\boldsymbol{\nu}}_1\|_2 &\lesssim \lambda_n^{-1} \{n_1^{-\frac{1}{p+1}} \log n_1 + (p+1)^{\frac{3}{2}} n_1^{-\frac{2}{p+1}} \log n_1\} + \sqrt{p} \mathbb{E}[d(\hat{\boldsymbol{\theta}}_1, \Theta)]. \end{aligned}$$

Step 4. Determine tuning parameter λ .

Note that the convergence rate of the first two terms in the right hand side of the above

inequalities cannot be determined when $p = o(\log n_1)$, because

$$\log \left(\frac{n_1^{-\frac{1}{p+1}} \log n_1}{(p+1)^{\frac{3}{2}} n_1^{-\frac{2}{p+1}} \log n_1} \right) = \log \left(\frac{n_1^{\frac{1}{p+1}}}{(p+1)^{\frac{3}{2}}} \right) = \frac{\log n_1}{p+1} - \frac{3}{2} \log(p+1), \quad (26)$$

where the two terms both converge to positive infinity as $n_1 \rightarrow \infty$. To simplify calculation, we assume that $p = o(\log^c n_1)$ with $0 < c < 1$, so that (26) goes to positive infinity as

$$\begin{aligned} \frac{\log n_1}{p+1} - \frac{3}{2} \log(p+1) &= \frac{\log n_1}{o(1) \log^c n_1 + 1} - \frac{3}{2} \log(o(\log^c n_1) + 1) \\ &= \frac{\log^{1-c} n_1}{o(1) + \log^{-c} n_1} - \frac{3}{2} \log(o(1) \log^c n_1 + 1) \rightarrow \infty, \text{ as } n_1 \rightarrow \infty, \end{aligned}$$

where the last equality holds because $\log^{1-c} n_1 \gg \log \log n_1$ for any $c \in (0, 1)$. Thus, the result can be reduced to

$$\mathbb{E}[d(\hat{\boldsymbol{\theta}}_1, \boldsymbol{\Theta})] \lesssim \left\{ n_1^{-\frac{1}{p+1}} \log n_1 + (\lambda_n \sqrt{p})^{\frac{a}{a-1}} \right\}^{\frac{1}{a}}, \quad \mathbb{E} \|\hat{\boldsymbol{\nu}}_1\|_2 \lesssim \lambda_n^{-1} n_1^{-\frac{1}{p+1}} \log n_1 + \sqrt{p} \mathbb{E}[d(\hat{\boldsymbol{\theta}}_1, \boldsymbol{\Theta})],$$

since the second term can be dominated by $n_1^{-\frac{1}{p+1}} \log n_1$. Further, when $\lambda = O(n_1^{-\frac{1}{2(p+1)}})$,

$$\begin{aligned} \mathbb{E}[d(\hat{\boldsymbol{\theta}}_1, \boldsymbol{\Theta})] &\lesssim \left\{ n_1^{-\frac{1}{p+1}} \log n_1 + n_1^{-\frac{a}{2(p+1)(a-1)}} \log^{\frac{ac}{2(a-1)}} n_1 \right\}^{\frac{1}{a}} \\ &\lesssim \left(n_1^{-\frac{1}{p+1}} \log^c n_1 \right)^{\frac{1}{2(a-1)}}, \\ &\lesssim \left(n_1^{-\frac{1}{p+1}} \log n_1 \right)^{\frac{1}{2(a-1)}} \\ &\rightarrow 0, \text{ as } n_1 \rightarrow \infty, \end{aligned}$$

where the third line holds because $\frac{a}{2(a-1)} < 1$ when $a > 2$, and the last line holds because

its logarithm converges to negative infinity when $c \in (0, 1)$, which is

$$\begin{aligned} \log \left(n_1^{-\frac{1}{p+1}} \log n_1 \right) &= \left\{ \log \log n_1 - \frac{\log n_1}{p+1} \right\} \lesssim \left\{ \log \log n_1 - \frac{\log n_1}{o(1) \log^c n_1 + 1} \right\} \\ &\lesssim \left\{ \log \log n_1 - \frac{\log^{1-c} n_1}{o(1) + \log^{-c} n_1} \right\} \rightarrow -\infty, \text{ as } n_1 \rightarrow \infty. \end{aligned}$$

Similarly, we can obtain

$$\begin{aligned} \mathbb{E} \|\hat{\boldsymbol{\nu}}_1\|_2 &\lesssim \lambda_n^{-1} n_1^{-\frac{1}{p+1}} \log n_1 + \sqrt{p} \mathbb{E}[d(\hat{\boldsymbol{\theta}}_1, \boldsymbol{\Theta})] \\ &\lesssim n_1^{\frac{1}{2(p+1)}} n_1^{-\frac{1}{p+1}} \log n_1 + \log^{c/2} n_1 \left(n_1^{-\frac{1}{p+1}} \log^c n_1 \right)^{\frac{1}{2(a-1)}} \\ &\lesssim n_1^{-\frac{1}{2(p+1)}} \log n_1 + n_1^{-\frac{1}{2(a-1)(p+1)}} \log n_1 \\ &\lesssim n_1^{-\frac{1}{2(a-1)(p+1)}} \log n_1. \end{aligned}$$

It converges to zero since its logarithm converges to negative infinity as well, which is

$$\begin{aligned} \log \left(n_1^{-\frac{1}{2(a-1)(p+1)}} \log n_1 \right) &= \log \log n_1 - \frac{\log n_1}{2(a-1)(p+1)} \lesssim \log \log n_1 - \frac{1}{2(a-1)} \frac{\log n_1}{o(1) \log^c n_1 + 1} \\ &\lesssim \log \log n_1 - \frac{1}{2(a-1)} \frac{\log^{1-c} n_1}{o(1) + \log^{-c} n_1} \rightarrow -\infty, \text{ as } n_1 \rightarrow \infty. \end{aligned}$$

A.4 Proof of Corollary 1

When p is fixed and $\lambda_n = O(n_1^{-\frac{1}{2(p+1)}})$,

$$\begin{aligned}
\mathbb{E}[d(\hat{\boldsymbol{\theta}}_1, \Theta)] &\lesssim \left\{ n_1^{-\frac{1}{p+1}} \log n_1 + (p+1)^{\frac{3}{2}} n_1^{-\frac{2}{p+1}} \log n_1 + (\lambda_n \sqrt{p})^{\frac{a}{a-1}} \right\}^{\frac{1}{a}} \\
&\lesssim \left\{ n_1^{-\frac{1}{p+1}} \log n_1 + \lambda_n^{\frac{a}{a-1}} \right\}^{\frac{1}{a}} \\
&= \left\{ n_1^{-\frac{1}{p+1}} \log n_1 + n_1^{-\frac{a}{2(p+1)(a-1)}} \right\}^{\frac{1}{a}} \\
&\lesssim \left(\frac{\log n_1}{n_1} \right)^{\frac{1}{2(p+1)(a-1)}}.
\end{aligned}$$

Similarly, we can obtain

$$\begin{aligned}
\mathbb{E}\|\hat{\boldsymbol{\nu}}_1\|_2 &\lesssim \lambda_n^{-1} n_1^{-\frac{1}{p+1}} \log n_1 + \mathbb{E}[d(\hat{\boldsymbol{\theta}}_1, \Theta)] \\
&\lesssim n_1^{\frac{1}{2(p+1)}} n_1^{-\frac{1}{p+1}} \log n_1 + \left(\frac{\log n_1}{n_1} \right)^{\frac{1}{2(p+1)(a-1)}} \\
&= n_1^{-\frac{1}{2(p+1)}} \log n_1 + \left(\frac{\log n_1}{n_1} \right)^{\frac{1}{2(p+1)(a-1)}} \\
&\lesssim \left(\frac{\log n_1}{n_1} \right)^{\frac{1}{2(p+1)(a-1)}}.
\end{aligned}$$

A.5 Proof of Corollary 2

Recall that for the estimate $\hat{\boldsymbol{\theta}}_1$ obtained in (1), $\mathbb{E}[d(\hat{\boldsymbol{\theta}}_1, \Theta)] = \|\hat{\boldsymbol{\theta}}_1 - \hat{\boldsymbol{\vartheta}}_1\|_2$, where $\hat{\boldsymbol{\vartheta}}_1 = \arg \min_{\boldsymbol{\vartheta} \in \Theta} \|\hat{\boldsymbol{\theta}}_1 - \boldsymbol{\vartheta}\|_2$. Let $\boldsymbol{w}_0(\hat{\boldsymbol{\theta}}_1) = (\hat{\boldsymbol{\mu}}_{\boldsymbol{\theta}_1}, \hat{\boldsymbol{\nu}}_{\boldsymbol{\theta}_1}, \hat{\boldsymbol{v}}_{\boldsymbol{\theta}_1})$ and $\boldsymbol{w}_0(\hat{\boldsymbol{\vartheta}}_1) = (\hat{\boldsymbol{\mu}}_{\boldsymbol{\vartheta}_1}, \hat{\boldsymbol{\nu}}_{\boldsymbol{\vartheta}_1}, \hat{\boldsymbol{v}}_{\boldsymbol{\vartheta}_1})$ be the first-layer weights of the generator networks $g_{\hat{\boldsymbol{\theta}}_1}$ and $g_{\hat{\boldsymbol{\vartheta}}_1}$, respectively. Then, from Corollary 1, when $\lambda_n = O(n_1^{-\frac{1}{2(p+1)}})$ and $p = o(\log^c n_1)$ with $c \in (0, 1)$,

$$\mathbb{E}\|\hat{\boldsymbol{\mu}}_{\boldsymbol{\theta}_1} - \hat{\boldsymbol{\mu}}_{\boldsymbol{\vartheta}_1}\|_2 \leq \mathbb{E}\|\hat{\boldsymbol{\theta}}_1 - \hat{\boldsymbol{\vartheta}}_1\|_2 = \mathbb{E}[d(\hat{\boldsymbol{\theta}}_1, \Theta)] \lesssim \left(n_1^{-\frac{1}{p+1}} \log n_1\right)^{\frac{1}{2(a-1)}}.$$

Lemma 6 shows that there exists a positive constant $c_\mu > 0$ such that $\|\hat{\boldsymbol{\mu}}_{\boldsymbol{\vartheta}}^{[j]}\|_2 \geq c_\mu$ for any $j = 1, \dots, p_s$ by the fact $\hat{\boldsymbol{\vartheta}} \in \Theta$. In other words, $\min_{1 \leq j \leq p_s} \|\hat{\boldsymbol{\mu}}_{\hat{\boldsymbol{\vartheta}}}^{[j]}\|_2 \geq c_\mu$. Then, for each $j = 1, \dots, p_s$,

$$\begin{aligned} c_\mu - \|\hat{\boldsymbol{\mu}}_{\hat{\boldsymbol{\theta}}_1}^{[j]}\|_2 &\leq \min_{1 \leq k \leq p_s} \|\hat{\boldsymbol{\mu}}_{\hat{\boldsymbol{\vartheta}}}^{[k]}\|_2 - \|\hat{\boldsymbol{\mu}}_{\hat{\boldsymbol{\theta}}_1}^{[j]}\|_2 \leq \|\hat{\boldsymbol{\mu}}_{\hat{\boldsymbol{\vartheta}}}^{[j]}\|_2 - \|\hat{\boldsymbol{\mu}}_{\hat{\boldsymbol{\theta}}_1}^{[j]}\|_2 \leq \left| \|\hat{\boldsymbol{\mu}}_{\hat{\boldsymbol{\theta}}_1}^{[j]}\|_2 - \|\hat{\boldsymbol{\mu}}_{\hat{\boldsymbol{\vartheta}}_1}^{[j]}\|_2 \right| \\ &\leq \|\hat{\boldsymbol{\mu}}_{\hat{\boldsymbol{\theta}}_1}^{[j]} - \hat{\boldsymbol{\mu}}_{\hat{\boldsymbol{\vartheta}}_1}^{[j]}\|_2 \leq \sum_{j=1}^{p_s} \|\hat{\boldsymbol{\mu}}_{\hat{\boldsymbol{\theta}}_1}^{[j]} - \hat{\boldsymbol{\mu}}_{\hat{\boldsymbol{\vartheta}}_1}^{[j]}\|_2 \leq \sqrt{p_s} \|\hat{\boldsymbol{\mu}}_{\boldsymbol{\theta}_1} - \hat{\boldsymbol{\mu}}_{\boldsymbol{\vartheta}_1}\|_2 \leq \sqrt{p_s} \|\hat{\boldsymbol{\theta}}_1 - \hat{\boldsymbol{\vartheta}}_1\|_2, \end{aligned}$$

indicating that $\|\hat{\boldsymbol{\mu}}_{\hat{\boldsymbol{\theta}}_1}^{[j]}\|_2 \geq c_\mu - \sqrt{p_s} \|\hat{\boldsymbol{\theta}}_1 - \hat{\boldsymbol{\vartheta}}_1\|_2$.

By Markov's inequality, for any positive constant $0 < c_0 < c_\mu / \sqrt{p_s}$,

$$P(\|\hat{\boldsymbol{\theta}}_1 - \hat{\boldsymbol{\vartheta}}_1\|_2 \leq c_0) = 1 - P(\|\hat{\boldsymbol{\theta}}_1 - \hat{\boldsymbol{\vartheta}}_1\|_2 \geq c_0) \geq 1 - \frac{\mathbb{E}\|\hat{\boldsymbol{\theta}}_1 - \hat{\boldsymbol{\vartheta}}_1\|_2}{c_0}.$$

Theorem 1 provides that there exists a positive constant c_1 such that

$$\mathbb{E}\|\hat{\boldsymbol{\theta}}_1 - \hat{\boldsymbol{\vartheta}}_1\|_2 \leq c_1 \left(n_1^{-\frac{1}{p+1}} \log n_1\right)^{\frac{1}{2(a-1)}},$$

so that for any $j = 1, \dots, p_s$,

$$P\left(\|\hat{\boldsymbol{\mu}}_{\boldsymbol{\theta}_1}^{[j]}\|_2 \geq c_\mu - \sqrt{p_s}c_0\right) \geq 1 - \frac{\mathbb{E}\|\hat{\boldsymbol{\theta}}_1 - \hat{\boldsymbol{\vartheta}}_1\|_2}{c_0} \geq 1 - \frac{c_1}{c_0} \left(n_1^{-\frac{1}{p+1}} \log n_1\right)^{\frac{1}{2(a-1)}}, \quad (27)$$

where $a > 2$ is a constant, independent of p and n_1 . For the part connecting the unimportant variables, by Theorem 1, for each $j = 1, \dots, p_c$,

$$P\left(\|\hat{\boldsymbol{\nu}}_{\boldsymbol{\theta}_1}^{[j]}\|_2 \geq c_\mu - \sqrt{p_s}c_0\right) \leq \frac{\mathbb{E}\|\hat{\boldsymbol{\nu}}_{\boldsymbol{\theta}_1}^{[j]}\|_2}{c_\mu - \sqrt{p_s}c_0} \leq \frac{c_2 n_1^{-\frac{1}{2(a-1)(p+1)}} \log n_1}{c_\mu - \sqrt{p_s}c_0}, \quad (28)$$

where $c_\mu - \sqrt{p_s}c_0 > 0$ by the constricton of Markov's inequality, and $c_2 > 0$ is a positive constant independent of p and n . Taking (27) and (28) together into consideration, for any $j = 1, \dots, p_s$ and $k = 1, \dots, p_c$,

$$\begin{aligned} & P\left(\{\|\hat{\boldsymbol{\mu}}_{\boldsymbol{\theta}_1}^{[j]}\|_2 \geq c_\mu - \sqrt{p_s}c_0\} \cap \{\|\hat{\boldsymbol{\nu}}_{\boldsymbol{\theta}_1}^{[k]}\|_2 \leq c_\mu - \sqrt{p_s}c_0\}\right) \\ &= P\left(\|\hat{\boldsymbol{\mu}}_{\boldsymbol{\theta}_1}^{[j]}\|_2 \geq c_\mu - \sqrt{p_s}c_0\right) - P\left(\{\|\hat{\boldsymbol{\mu}}_{\boldsymbol{\theta}_1}^{[j]}\|_2 \geq c_\mu - \sqrt{p_s}c_0\} \cap \{\|\hat{\boldsymbol{\nu}}_{\boldsymbol{\theta}_1}^{[k]}\|_2 \geq c_\mu - \sqrt{p_s}c_0\}\right) \\ &\geq P\left(\|\hat{\boldsymbol{\mu}}_{\boldsymbol{\theta}_1}^{[j]}\|_2 \geq c_\mu - \sqrt{p_s}c_0\right) - P\left(\|\hat{\boldsymbol{\nu}}_{\boldsymbol{\theta}_1}^{[k]}\|_2 \geq c_\mu - \sqrt{p_s}c_0\right) \\ &\geq 1 - \frac{c_1}{c_0} \left(n_1^{-\frac{1}{p+1}} \log n_1\right)^{\frac{1}{2(a-1)}} - \frac{c_2}{c_\mu - \sqrt{p_s}c_0} n_1^{-\frac{1}{2(a-1)(p+1)}} \log n_1 \\ &\geq 1 - 2 \max\left\{\frac{c_1}{c_0}, \frac{c_2}{c_\mu - \sqrt{p_s}c_0}\right\} n_1^{-\frac{1}{2(a-1)(p+1)}} \log n_1 \\ &\rightarrow 1, \text{ as } n_1 \rightarrow \infty, \end{aligned}$$

since $n_1^{-\frac{1}{2(a-1)(p+1)}} \log n_1$ converges to zero as $n_1 \rightarrow \infty$.

A.6 Proof of Theorem 2

Consider the Wasserstein distance between $P_{\hat{\mathbf{X}}^s, g_{\hat{\theta}_2}}$ and $P_{\mathbf{X}^s, Y}$,

$$\begin{aligned} & \mathbb{E}W(P_{\hat{\mathbf{X}}^s, g_{\hat{\theta}_2}}, P_{\mathbf{X}^s, Y}) \\ &= \mathbb{E} \sup_{f \in \mathcal{F}_{\text{Lip}}^1} \left\{ \mathbb{E}_{\hat{\mathbf{X}}^s, \mathbf{Z}} f(\hat{\mathbf{X}}^s, g_{\hat{\theta}_2}(\hat{\mathbf{X}}^s, \mathbf{Z})) - \mathbb{E}_{\hat{\mathbf{X}}^s, Y} f(\hat{\mathbf{X}}^s, Y) + \mathbb{E}_{\hat{\mathbf{X}}^s, Y} f(\hat{\mathbf{X}}^s, Y) - \mathbb{E}_{\mathbf{X}^s, Y} f(\mathbf{X}^s, Y) \right\} \\ &\leq \mathbb{E} \sup_{f \in \mathcal{F}_{\text{Lip}}^1} \left\{ \mathbb{E}_{\hat{\mathbf{X}}^s, \mathbf{Z}} f(\hat{\mathbf{X}}^s, g_{\hat{\theta}_2}(\hat{\mathbf{X}}^s, \mathbf{Z})) - \mathbb{E}_{\hat{\mathbf{X}}^s, Y} f(\hat{\mathbf{X}}^s, Y) \right\} + \mathbb{E} \sup_{f \in \mathcal{F}_{\text{Lip}}^1} \left\{ \mathbb{E}_{\hat{\mathbf{X}}^s, Y} f(\hat{\mathbf{X}}^s, Y) - \mathbb{E}_{\mathbf{X}^s, Y} f(\mathbf{X}^s, Y) \right\}. \end{aligned}$$

Corollary 2 shows that $\hat{\mathbf{X}}^s = \mathbf{X}^s$ with probability $1 - c_{p_s} n_1^{-\frac{1}{2(\alpha-1)(p+1)}} \log n_1$, so that in the same probability, $\mathbb{E} \sup_{f \in \mathcal{F}_{\text{Lip}}^1} \left\{ \mathbb{E}_{\hat{\mathbf{X}}^s, Y} f(\hat{\mathbf{X}}^s, Y) - \mathbb{E}_{\mathbf{X}^s, Y} f(\mathbf{X}^s, Y) \right\} = 0$. Therefore, we only focus on the first term, which can be decomposed as:

$$\begin{aligned} & \mathbb{E} \sup_{f \in \mathcal{F}_{\text{Lip}}^1} \left\{ \mathbb{E}_{\hat{\mathbf{X}}^s, \mathbf{Z}} f(\hat{\mathbf{X}}^s, g_{\hat{\theta}_2}(\hat{\mathbf{X}}^s, \mathbf{Z})) - \mathbb{E}_{\hat{\mathbf{X}}^s, Y} f(\hat{\mathbf{X}}^s, Y) \right\} \\ &= \mathbb{E} \sup_{f \in \mathcal{F}_{\text{Lip}}^1} \left\{ \mathbb{E}_{\hat{\mathbf{X}}^s, \mathbf{Z}} f(\hat{\mathbf{X}}^s, g_{\hat{\theta}_2}(\hat{\mathbf{X}}^s, \mathbf{Z})) - \frac{1}{n_2} \sum_{i=1}^{n_2} f(\hat{\mathbf{X}}_i^s, g_{\hat{\theta}_2}(\hat{\mathbf{X}}_i^s, \mathbf{Z}_i)) \right. \\ &\quad \left. + \frac{1}{n_2} \sum_{i=1}^{n_2} f(\hat{\mathbf{X}}_i^s, g_{\hat{\theta}_2}(\hat{\mathbf{X}}_i^s, \mathbf{Z}_i)) - \frac{1}{n_2} \sum_{i=1}^{n_2} f(\hat{\mathbf{X}}_i^s, Y_i) + \frac{1}{n_2} \sum_{i=1}^{n_2} f(\hat{\mathbf{X}}_i^s, Y_i) - \mathbb{E}_{\hat{\mathbf{X}}^s, Y} f(\hat{\mathbf{X}}^s, Y) \right\} \\ &\leq \mathbb{E} \sup_{f \in \mathcal{F}_{\text{Lip}}^1} \left\{ \mathbb{E}_{\hat{\mathbf{X}}^s, \mathbf{Z}} f(\hat{\mathbf{X}}^s, g_{\hat{\theta}_2}(\hat{\mathbf{X}}^s, \mathbf{Z})) - \frac{1}{n_2} \sum_{i=1}^{n_2} f(\hat{\mathbf{X}}_i^s, g_{\hat{\theta}_2}(\hat{\mathbf{X}}_i^s, \mathbf{Z}_i)) \right\} \\ &\quad + \mathbb{E} \sup_{f \in \mathcal{F}_{\text{Lip}}^1} \left\{ \frac{1}{n_2} \sum_{i=1}^{n_2} f(\hat{\mathbf{X}}_i^s, g_{\hat{\theta}_2}(\hat{\mathbf{X}}_i^s, \mathbf{Z}_i)) - \frac{1}{n_2} \sum_{i=1}^{n_2} f(\hat{\mathbf{X}}_i^s, Y_i) \right\} \\ &\quad + \mathbb{E} \sup_{f \in \mathcal{F}_{\text{Lip}}^1} \left\{ \frac{1}{n_2} \sum_{i=1}^{n_2} f(\hat{\mathbf{X}}_i^s, Y_i) - \mathbb{E}_{\hat{\mathbf{X}}^s, Y} f(\hat{\mathbf{X}}^s, Y) \right\}. \end{aligned}$$

Similar to the results in Lemmas 1-2, the first and third terms above have their upper bounds as follows:

$$\begin{aligned} \mathbb{E} \sup_{f \in \mathcal{F}_{\text{Lip}}^1} \left\{ \mathbb{E}_{\hat{\mathbf{X}}^s, \mathbf{Z}} f(\hat{\mathbf{X}}^s, g_{\hat{\theta}_2}(\hat{\mathbf{X}}^s, \mathbf{Z})) - \frac{1}{n_2} \sum_{i=1}^{n_2} f(\hat{\mathbf{X}}_i^s, g_{\hat{\theta}_2}(\hat{\mathbf{X}}_i^s, \mathbf{Z}_i)) \right\} &\lesssim n_2^{\frac{1}{p_s+1}} \log n_2, \\ \mathbb{E} \sup_{f \in \mathcal{F}_{\text{Lip}}^1} \left\{ \frac{1}{n_2} \sum_{i=1}^{n_2} f(\hat{\mathbf{X}}_i^s, Y_i) - \mathbb{E}_{\hat{\mathbf{X}}^s, Y} f(\hat{\mathbf{X}}^s, Y) \right\} &\lesssim \sqrt{p_s + 1} n_2^{-\frac{1}{p_s+1}}. \end{aligned}$$

Then, when the second stage's network classes \mathcal{F}_{ϕ_2} and \mathcal{G}_{θ_2} satisfy Conditions 5 and 4,

$$\begin{aligned} &\mathbb{E} \sup_{f \in \mathcal{F}_{\text{Lip}}^1} \left\{ \frac{1}{n_2} \sum_{i=1}^{n_2} f(\hat{\mathbf{X}}_i^s, g_{\hat{\theta}_2}(\hat{\mathbf{X}}_i^s, \mathbf{Z}_i)) - \frac{1}{n_2} \sum_{i=1}^{n_2} f(\hat{\mathbf{X}}_i^s, Y_i) \right\} \\ &\leq 2 \sup_{f \in \mathcal{F}_{\text{Lip}}^1} \inf_{f_{\phi_2} \in \mathcal{F}_{\phi_2}} \|f - f_{\phi_2}\| + \inf_{g_{\theta_2} \in \mathcal{G}_{\theta_2}} \sup_{f_{\phi_2} \in \mathcal{F}_{\phi_2}} \left\{ \frac{1}{n_2} \sum_{i=1}^{n_2} f(\hat{\mathbf{X}}_i^s, g_{\theta_2}(\hat{\mathbf{X}}_i^s, \mathbf{Z}_i)) - \frac{1}{n_2} \sum_{i=1}^{n_2} f(\hat{\mathbf{X}}_i^s, Y_i) \right\} \\ &\leq 2 \sup_{f \in \mathcal{F}_{\text{Lip}}^1} \inf_{f_{\phi_2} \in \mathcal{F}_{\phi_2}} \|f - f_{\phi_2}\| \leq 76(p_s + 1)^{3/2} n_2^{-\frac{2}{p_s+1}} \log n_2 \lesssim n_2^{-\frac{2}{p_s+1}} \log n_2, \end{aligned}$$

where the second and third lines hold by Lemma C.1 and Lemma C.3 in Liu et al. (2021), the fourth line holds by (20), and the last line holds as p_s is fixed.

A.7 Proof of Proposition 1

Suppose that Conditions 7 and 8 hold. Then, according to Theorem 1.1 in Stute (1996), for any $(x, t) \in \mathbb{R}^{d \times 1}$,

$$\mathbb{E}|\hat{F}_{XT}(x, t) - F_{XT}(x, t)| \leq 2F_{XT}(x, t).$$

Condition 1 guarantees that $M_3 = \mathbb{E}_{X,T}|(X, T)|^3 < \infty$. Last, following Theorem 3.1 in Lei (2020),

$$\mathbb{E}W(\hat{F}_{X,T}, F_{X,T}) \leq Cn^{-\frac{1}{d+1}},$$

where C is a positive constant depending on M_3 .

A.8 Computational algorithm for the penalized WGAN for censored survival data

Algorithm 2 Penalized WGAN for censored survival data

Require: Tuning parameter λ_n ; Minibatch size $v \leq n_1$; Clipping parameter c ; Noise dimension m ; Learning rates α_f, α_g .

- 1: **for** number of training iterations in stage 1 **do**
- 2: Sample $\{(\mathbf{x}_{bj}, y_{bj}, \Delta_{bj})\}_{j=1}^{n_b}$ from $\{(\mathbf{x}_i, y_i, \Delta_i)\}_{i=1}^{n_1}$, and noise $\{\mathbf{z}_j\}_{j=1}^{n_b}$ from $N(\mathbf{0}, \mathbf{I}_m)$.
- 3: Order the samples as $y_{(b1)} \leq y_{(b2)} \leq \dots \leq y_{(bn_b)}$, and denote $\mathbf{x}_{(b1)}, \dots, \mathbf{x}_{(bn_b)}$ and $\Delta_{(b1)}, \dots, \Delta_{(bn_b)}$ as the predictors and indicators corresponding to the ordered y_{bj} 's.
- 4: Compute the Kaplan-Meier weights as

$$\omega_{(b1)} = \frac{\Delta_{(b1)}}{n_b}, \quad \omega_{(bj)} = \frac{\Delta_{(j)}}{n_b - j + 1} \prod_{k=1}^{j-1} \left(\frac{n_b - k}{n - k + 1} \right)^{\Delta_{(k)}}, \quad j = 2, \dots, n_b.$$

- 5: Update the discriminator f_{ϕ_1} by ascending its stochastic gradient:

$$f_{\phi_1} \leftarrow \nabla_{\phi_1} \left[\frac{1}{n_b} \sum_{j=1}^{n_b} f_{\phi_1}(\mathbf{x}_{bj}, g_{\theta}(\mathbf{x}_{bj}, \mathbf{z}_j)) - \sum_{j=1}^{n_b} \omega_{(bj)} f_{\phi_1}(\mathbf{x}_{(bj)}, y_{(bj)}) \right],$$

$$\phi_1 \leftarrow \phi_1 + \alpha_f \cdot \text{RMSPProp}(\phi_1, f_{\phi_1}), \quad \phi_1 \leftarrow \text{clip}(\phi_1, -c, c).$$

- 6: Update the generator g_{θ_1} by descending its stochastic gradient:

$$g_{\theta_1} \leftarrow \nabla_{\theta} \left[\frac{1}{n_b} \sum_{j=1}^{n_b} f_{\phi_1}(\mathbf{x}_{bj}, g_{\theta_1}(\mathbf{x}_{bj}, \mathbf{z}_j)) + \lambda_n \sum_{l=1}^p \|\mathbf{w}_0(\theta_1)^{[l,j]}\|_2 \right],$$

$$\theta \leftarrow \theta - \alpha_g \cdot \text{RMSPProp}(\theta, g_{\theta_1}).$$

- 7: **end for**
-

A.9 Additional simulation study details

A.9.1 Additional simulation results for $p_s = 30$: Distribution estimation

Beyond those evaluated in the main text, as a “byproduct”, the proposed approach can also provide the conditional distribution estimation. For comparison, we also apply the conditional WGAN (cWGAN, Liu et al., 2021) with the original high-dimensional predictors and the set of important predictors, respectively – here the latter is an oracle approach and is not feasible in practice. To evaluate the conditional distribution estimation, we consider the mean squared error (MSE) of the estimated mean $\mathbb{E}(Y|\mathbf{X})$, the estimated conditional standard deviation $SD(Y|\mathbf{X})$, and the estimated conditional quantile of level τ , $F_{Y|\mathbf{X}}^{-1}(\tau|\mathbf{X})$, which are defined as:

$$\begin{aligned} \text{MSE}(\text{mean}) &= \frac{1}{T} \sum_{i=1}^T \{\widehat{\mathbb{E}}(Y | \mathbf{X} = \mathbf{x}_i) - \mathbb{E}(Y | \mathbf{X} = \mathbf{x}_i)\}^2, \\ \text{MSE}(\text{sd}) &= \frac{1}{T} \sum_{i=1}^T \{\widehat{SD}(Y | \mathbf{X} = \mathbf{x}_i) - SD(Y | \mathbf{X} = \mathbf{x}_i)\}^2, \\ \text{MSE}(\tau) &= \frac{1}{T} \sum_{i=1}^T \left\{ \widehat{F}_{Y|\mathbf{X}}^{-1}(\tau | \mathbf{X} = \mathbf{x}_i) - F_{Y|\mathbf{X}}^{-1}(\tau | \mathbf{X} = \mathbf{x}_i) \right\}^2, \end{aligned}$$

where T is the size of testing data, $\widehat{\mathbb{E}}(Y|\mathbf{X} = \mathbf{x}_i) = J^{-1} \sum_{j=1}^J \hat{g}_\gamma(\mathbf{x}_i, \mathbf{Z}_{ij})$, $\widehat{SD}(Y|\mathbf{X} = \mathbf{x}_i) = [J^{-1} \sum_{j=1}^J \{\hat{g}_\theta(\mathbf{x}_i, \mathbf{Z}_{ij}) - \widehat{\mathbb{E}}(Y|\mathbf{X} = \mathbf{x}_i)\}^2]^{1/2}$, and $F_{Y|\mathbf{X}}^{-1}(\tau|\mathbf{X} = \mathbf{x}_i)$ is the τ -th conditional quantile for a given $\mathbf{X} = \mathbf{x}_i$. The noise vector \mathbf{Z} is generated from $N(\mathbf{0}, \mathbf{I}_5)$, and $J = 500$. Table A.3 summarizes the average MSEs and the corresponding standard errors in parentheses. It can be seen that the MSEs of the proposed approach are smaller than cWGAN in all models. Further, they remain stable with the increasing dimension of \mathbf{X} .

Table A.3: Mean squared error (MSE) of the estimated conditional mean, the estimated conditional standard deviation, and the estimated conditional quantile of level τ for M1 to M4 with $p_s = 30$.

Method	p	Mean	Sd	τ			
				0.25	0.50	0.75	
M1	Oracle	30	0.34(0.07)	0.13(0.07)	0.40(0.08)	0.35(0.07)	0.41(0.09)
	Proposed	100	0.52(0.08)	0.21(0.09)	0.63(0.13)	0.53(0.08)	0.61(0.12)
		300	0.50(0.08)	0.28(0.15)	0.61(0.12)	0.51(0.08)	0.66(0.11)
		500	0.56(0.11)	0.29(0.12)	0.64(0.18)	0.49(0.11)	0.59(0.14)
		1000	0.56(0.14)	0.19(0.13)	0.65(0.16)	0.57(0.15)	0.66(0.18)
	cWGAN	100	0.66(0.11)	0.86(0.14)	1.09(0.15)	0.66(0.11)	1.02(0.12)
		300	2.23(0.28)	0.91(0.03)	2.52(0.29)	2.23(0.28)	2.77(0.39)
		500	4.79(0.49)	0.90(0.02)	5.28(0.64)	4.80(0.56)	5.14(0.53)
		1000	12.21(0.80)	0.89(0.02)	12.67(0.88)	12.21(0.80)	12.56(0.90)
	M2	Oracle	30	-	-	2.75(3.02)	2.52(2.70)
Proposed		100	-	-	3.62(3.37)	2.96(3.19)	4.55(5.79)
		300	-	-	5.92(5.04)	3.31(2.81)	3.88(3.31)
		500	-	-	5.22(4.97)	2.70(2.49)	4.02(3.58)
		1000	-	-	7.15(6.65)	2.74(1.94)	2.74(2.64)
cWGAN		100	-	-	26.86(12.34)	26.38(10.78)	26.49(10.05)
		300	-	-	32.66(15.01)	30.73(12.93)	32.66(13.90)
		500	-	-	32.13(19.67)	30.29(19.07)	30.08(18.86)
		1000	-	-	32.40(11.78)	32.35(10.97)	34.05(10.56)
M3		Oracle	30	0.97(0.35)	0.78(0.16)	1.07(0.34)	0.97(0.35)
	Proposed	100	1.19(0.28)	0.85(0.12)	1.32(0.27)	1.19(0.28)	1.27(0.28)
		300	1.15(0.28)	0.85(0.13)	1.28(0.26)	1.15(0.28)	1.23(0.29)
		500	1.16(0.31)	0.83(0.19)	1.27(0.31)	1.17(0.32)	1.27(0.31)
		1000	1.22(0.36)	0.85(0.11)	1.34(0.33)	1.22(0.36)	1.31(0.37)
	cWGAN	100	1.87(0.24)	0.91(0.04)	1.99(0.24)	1.87(0.24)	1.97(0.24)
		300	5.53(0.43)	0.84(0.06)	5.61(1.36)	5.53(1.43)	5.65(1.60)
		500	8.32(0.90)	0.85(0.05)	8.38(0.85)	8.32(0.90)	8.47(0.98)
		1000	17.62(0.68)	0.88(0.03)	17.62(0.72)	17.62(0.72)	17.82(0.69)
	M4	Oracle	30	0.29(0.14)	0.29(0.07)	0.56(0.16)	0.38(0.17)
Proposed		100	0.40(0.22)	0.71(0.58)	1.09(0.44)	0.53(0.29)	1.08(0.78)
		300	0.50(0.24)	0.56(0.76)	1.19(0.57)	0.73(0.39)	1.05(0.46)
		500	0.54(0.30)	0.86(0.62)	1.21(0.45)	0.84(0.44)	1.35(0.55)
		1000	0.41(0.15)	0.70(0.73)	0.93(0.26)	0.65(0.27)	1.08(0.33)
cWGAN		100	0.57(0.17)	0.44(0.15)	1.10(0.35)	0.91(0.36)	1.23(0.53)
		300	0.85(0.56)	1.58(0.49)	3.21(0.74)	0.85(0.44)	3.06(0.86)
		500	0.94(0.82)	8.55(0.67)	4.33(0.36)	0.80(0.31)	4.34(0.38)
		1000	0.90(0.87)	8.19(0.34)	4.19(0.65)	0.68(0.45)	3.93(0.32)

Note: In M2, the conditional distribution $P_{Y|X}$ is a t -distribution with degree of freedom 1, and the mean and standard deviation are not well defined.

A.9.2 Simulation results for $p_s = 5$

We consider the same models as in Section 5 but set $\beta = (\mathbf{I}_5, \mathbf{I}_{p_c})$. The predictors \mathbf{X} are generated from $N(\mathbf{0}, \mathbf{I}_p)$ with $p \in \{100, 300, 500, 1000\}$, and the noise $\mathbf{Z} \sim N(\mathbf{0}, \mathbf{I}_5)$. All methods adopt FNNs with two hidden layers, and the numbers of nodes are set as 64 and 32. For M1 and M3, $n = 1,000$; For M2, $n = 10,000$; For M4, $n = 2,000$; And for M5 and M6, $n = 5,000$. Table A.4 summarizes the variable selection and prediction results, and Table A.5 summarizes the condition distribution estimation results. The observed patterns and superiority of the proposed approach are similar to those for $\mathbf{X}^s \in \mathbb{R}^{30}$.

Table A.4: Simulation results for variable selection and prediction with $p_s = 5$.

p	Proposed			P-LS			DFS			LassoNet			GCRNet			
	MSE/C-idx	TPR	FPR													
M1	100	1.08(0.04)	1.00	0.00	1.04(0.03)	1.00	0.00	1.10(0.07)	1.00	0.00	1.03(0.03)	1.00	0.00	1.06(0.03)	1.00	0.00
	300	1.08(0.07)	1.00	0.00	1.08(0.07)	1.00	0.00	1.22(0.30)	1.00	0.00	1.04(0.04)	1.00	0.00	1.08(0.11)	1.00	0.00
	500	1.05(0.10)	1.00	0.00	1.11(0.07)	1.00	0.00	1.66(0.64)	0.94	0.00	1.05(0.05)	1.00	0.00	1.12(0.20)	1.00	0.00
	1000	1.07(0.05)	1.00	0.00	1.11(0.07)	1.00	0.00	1.59(0.65)	0.93	0.00	1.05(0.05)	1.00	0.00	1.10(0.13)	1.00	0.00
M2	100	-	1.00	0.00	-	0.56	0.48	-	0.10	0.05	-	1.0	0.19	-	0.20	0.04
	300	-	1.00	0.00	-	0.49	0.49	-	0.04	0.02	-	1.0	0.20	-	0.16	0.19
	500	-	1.00	0.00	-	0.46	0.51	-	0.00	0.00	-	1.0	0.14	-	0.00	0.00
	1000	-	0.98	0.00	-	0.64	0.50	-	0.00	0.00	-	1.0	0.24	-	0.00	0.00
M3	100	1.13(0.36)	1.00	0.00	0.54(0.29)	1.00	0.00	1.40(0.26)	1.00	0.00	0.60(0.12)	1.00	0.00	0.69(0.34)	1.00	0.00
	300	1.17(0.32)	1.00	0.00	0.64(0.34)	1.00	0.00	1.47(0.40)	1.00	0.00	0.72(0.28)	1.00	0.00	0.78(0.47)	1.00	0.00
	500	1.04(0.29)	1.00	0.00	0.96(0.79)	1.00	0.00	1.69(0.54)	0.96	0.00	0.61(0.08)	1.00	0.00	0.70(0.47)	1.00	0.00
	1000	1.10(0.28)	1.00	0.00	0.97(0.94)	1.00	0.00	1.55(0.43)	0.96	0.00	0.66(0.14)	1.00	0.00	0.63(0.39)	1.00	0.00
M4	100	2.42(0.17)	1.00	0.00	2.09(0.18)	0.62	0.50	2.41(0.22)	0.04	0.05	2.00(0.14)	1.00	0.00	2.19(0.27)	0.04	0.00
	300	2.59(0.23)	1.00	0.00	2.46(0.33)	0.49	0.49	2.42(0.27)	0.02	0.02	2.11(0.11)	1.00	0.00	2.18(0.19)	0.02	0.00
	500	2.50(0.16)	1.00	0.00	2.42(0.25)	0.46	0.51	2.42(0.24)	0.04	0.01	2.06(0.18)	1.00	0.00	2.78(0.30)	0.00	0.00
	1000	2.41(0.27)	1.00	0.00	2.65(0.35)	0.64	0.50	2.74(0.24)	0.04	0.00	2.70(0.16)	1.00	0.00	2.74(0.31)	0.00	0.00
M5	100	0.79(0.01)	1.00	0.00	0.79(0.01)	1.00	0.00	-	-	-	0.87(0.01)	1.00	0.00	0.65(0.01)	1.00	0.36
	300	0.79(0.01)	1.00	0.00	0.79(0.01)	1.00	0.00	-	-	-	0.83(0.06)	0.98	0.00	0.77(0.10)	1.00	0.30
	500	0.79(0.01)	1.00	0.00	0.79(0.01)	1.00	0.00	-	-	-	0.77(0.04)	0.88	0.01	0.65(0.01)	1.00	0.07
	1000	0.79(0.01)	1.00	0.00	0.79(0.01)	1.00	0.00	-	-	-	0.74(0.05)	0.62	0.00	0.80(0.06)	1.00	0.03
M6	100	0.73(0.01)	1.00	0.00	0.64(0.01)	1.00	0.00	-	-	-	0.71(0.01)	0.90	0.00	0.60(0.02)	0.20	0.00
	300	0.73(0.01)	0.98	0.00	0.62(0.02)	0.64	0.00	-	-	-	0.71(0.01)	0.44	0.00	0.59(0.01)	0.20	0.00
	500	0.73(0.02)	1.00	0.02	0.62(0.01)	0.52	0.00	-	-	-	0.71(0.02)	0.40	0.00	0.59(0.01)	0.20	0.00
	1000	0.71(0.09)	1.00	0.09	0.60(0.02)	0.50	0.00	-	-	-	0.70(0.02)	0.52	0.00	0.50(0.03)	0.00	0.00

Note: The standard errors for MSE are given in parentheses; With DFS, the number of variables to be selected is set as 5, which is required during the training process.

Table A.5: Mean squared error (MSE) of the estimated conditional mean, the estimated conditional standard deviation, and the estimated conditional quantile of level τ for M1 to M4 with $p_s = 5$.

Method	p	Mean	Sd	τ			
				0.25	0.50	0.75	
M1	Oracle	5	0.07(0.03)	0.03(0.03)	0.10(0.06)	0.09(0.06)	0.11(0.07)
	Proposed	100	0.08(0.03)	0.04(0.03)	0.11(0.05)	0.10(0.04)	0.12(0.05)
		300	0.07(0.03)	0.03(0.01)	0.08(0.02)	0.08(0.03)	0.10(0.04)
		500	0.06(0.02)	0.03(0.01)	0.08(0.02)	0.07(0.03)	0.09(0.04)
		1000	0.06(0.01)	0.02(0.01)	0.08(0.02)	0.08(0.02)	0.09(0.03)
	cWGAN	100	0.45(0.08)	0.39(0.37)	0.65(0.24)	0.46(0.08)	0.62(0.20)
		300	0.75(0.08)	0.95(0.02)	1.20(0.11)	0.75(0.08)	1.16(0.14)
		500	1.25(0.11)	0.95(0.01)	1.73(0.20)	1.25(0.11)	1.63(0.26)
		1000	2.35(0.11)	0.94(0.02)	2.79(0.34)	2.35(0.11)	2.77(0.27)
	M2	Oracle	5	-	-	2.69(2.41)	2.07(1.72)
Proposed		100	-	-	2.28(2.36)	2.24(2.21)	2.14(2.23)
		300	-	-	2.87(2.94)	2.12(2.06)	2.67(1.74)
		500	-	-	3.36(1.96)	1.90(2.13)	4.44(3.44)
		1000	-	-	3.83(1.51)	1.93(2.17)	4.46(5.78)
cWGAN		100	-	-	4.07(2.05)	2.76(1.08)	4.35(2.32)
		300	-	-	5.10(2.32)	4.04(2.10)	4.67(2.06)
		500	-	-	5.87(2.30)	4.70(2.63)	5.38(2.74)
		1000	-	-	5.62(2.72)	5.50(2.89)	5.39(4.37)
M3		Oracle	5	0.73(0.23)	0.71(0.13)	0.80(0.22)	0.73(0.23)
	Proposed	100	0.73(0.23)	0.71(0.13)	0.80(0.22)	0.73(0.23)	0.83(0.23)
		300	0.71(0.22)	0.78(0.11)	0.78(0.22)	0.71(0.22)	0.78(0.23)
		500	0.77(0.29)	0.78(0.23)	0.89(0.23)	0.83(0.23)	0.90(0.24)
		1000	0.79(0.29)	0.73(0.13)	0.99(0.31)	0.75(0.32)	0.87(0.32)
	cWGAN	100	1.37(0.23)	0.94(0.12)	1.51(0.24)	1.37(0.23)	1.46(0.22)
		300	3.49(0.99)	0.95(0.22)	3.59(0.97)	3.49(0.99)	3.61(1.02)
		500	4.96(0.83)	0.92(0.18)	5.01(1.44)	4.97(1.43)	5.14(1.44)
		1000	7.87(0.76)	0.90(0.33)	7.83(0.66)	7.87(0.67)	8.08(0.71)
	M4	Oracle	5	0.03(0.01)	0.03(0.01)	0.06(0.03)	0.04(0.01)
Proposed		100	0.05(0.04)	0.07(0.09)	0.13(0.06)	0.09(0.06)	0.14(0.07)
		300	0.03(0.01)	0.11(0.07)	0.14(0.07)	0.10(0.05)	0.12(0.05)
		500	0.08(0.05)	0.08(0.05)	0.12(0.07)	0.09(0.05)	0.11(0.06)
		1000	0.07(0.04)	0.08(0.09)	0.12(0.04)	0.09(0.05)	0.13(0.05)
cWGAN		100	0.08(0.05)	2.23(0.11)	1.03(0.07)	0.13(0.01)	1.06(0.07)
		300	0.07(0.05)	2.44(0.16)	1.18(0.10)	0.14(0.02)	1.13(0.07)
		500	0.08(0.05)	2.47(0.13)	1.18(0.11)	0.13(0.02)	1.12(0.09)
		1000	0.08(0.04)	2.67(0.09)	1.27(0.08)	0.15(0.04)	1.26(0.14)

Note: In M2, the conditional distribution $P_{Y|\mathbf{X}}$ is a t -distribution with degree of freedom 1, and the mean and standard deviation are not well defined.

A.10 Additional details for the data analysis

A.10.1 Settings of the neural networks

For comparability, we adopt similar network structures for all the methods. The neural networks used in the proposed approach, GCRNet, P-LS, LassoNet, and the approximation layers of DFS are two-layer FNNs with widthsh (64, 32) and the ReLu activation function. LassoNet has a single residual connection, and DFS has a selection layer. The noise vector used in the proposed approach is generated from the standard normal distribution with dimension 5. The batch size, learning rate, and value of tuning parameter λ_n are summarized in Table A.6.

Table A.6: Summary of network training settings.

	TCGA			MIMIC-III						HIV-1		
	batch	lr	λ_n	Albumin			Survival			batch	lr	λ_n
Proposed	200	1e-4	1e-4	50	1e-4	1e-6	128	5e-5	1e-5	25	1e-4	1e-5
P-LS	200	1e-5	0.1	50	1e-4	1	128	5e-5	0.5	25	0.01	0.1
DFS	360	1e-4	1	1933	0.1	1	-	-	-	-	0.1	1
LassoNet	360	1e-3	-	1933	1e-3	-	8323	1e-3	-	-	1e-3	-
GCRNet	300	1e-3	-	50	0.01	-	8323	0.001	-	50	1e-3	-

Note: λ_n in LassoNet and GCRNet are selected by cross-validation in each replication. The batch sizes in DFS and LassoNet vary since the sample sizes of the three drugs are different.

A.10.2 Details of the selected predictors

For the TCGA-LUAD data, Table A.7 presents the identified genes using the proposed and alternative methods. Those in bold are selected by multiple methods. No gene is identified by GCRNet. In Table A.8, we present the genes that are frequently selected (which are defined as being selected in at least half of the 30 replications). It is observed that DFS identifies quite different genes across the replications, and GCRNet does not identify any important genes in 27 out of the 30 replications.

For the analysis of the MIMIC-III data on albumin level, Table A.9 presents the important predictors identified by each method, and Table A.10 presents the frequencies of these

Table A.7: Analysis of the TCGA-LUAD data: identified important genes.

Method	Identified Genes
Proposed	ST6GAL1, ISL2, OR10G8, WDR89, OR4N5, TRIM16L, C1orf126, TMEM159, PIK3C2A
P-LS	PDE8A, SLC25A21, COL13A1, C18orf54, C1QTNF3, ST6GAL1, AIG1, MRPL28, RNPC3, ISL2, OR4N5, DEFB136, WDR89
DFS	AAMP, ATIC, C4orf29, CTU2, DCI, FLCN, HSD17B10, MADD, MYD88, PRODH, SCAI, SNCG, VSNL1, XAF1
LassoNet	ST6GAL1, ISL2, WDR89, OR4N5, OR10G8, TRIM16L, HAPLN2, C1orf126, PIK3C2A, H1FX, TAF2, ADRA2A, KPTN, TMEM63A, PTPRD, JHDM1D, MYL3, LANCL2, TXNDC3
GCRNet	-

Table A.8: Analysis of the TCGA-LUAD data: Frequently identified important genes and their identification frequencies.

Proposed	Gene	ISL2	OR10G8	OR4N5	SLC47A2	ST6GAL1	WDR89			
	Frequency	0.87	0.83	0.93	0.83	0.93	0.93			
P-LS	Gene	AFTPH	C1QTNF3	ISL2	OR10G8	OR4N5	ST6GAL1	TRIM16L	WDR89	
	Frequency	0.50	0.67	0.83	0.50	0.73	0.83	0.77	0.80	
DFS	Gene	-								
	Frequency	-								
LassoNet	Gene	GLOD4	H1FX	HAPLN2	ISL2	KPTN	LANCL2	MPPED2	OR10G8	OR4N5
	Frequency	0.57	0.60	0.70	0.90	0.77	0.50	0.50	0.77	0.90
GCRNet	Gene	PIK3C2A	PTPRD	ST6GAL1	TAF2	TMEM63A	TRIM16L	VPS13C	WDR89	
	Frequency	0.57	0.77	1.00	0.87	0.90	0.60	0.90	0.90	

predictors identified over the 30 replications.

For the analysis of the MIMIC-III data on survival, Table A.11 presents the important predictors identified by each method, and Figure A.2 presents the identification frequencies across the 30 replications.

For the analysis of the HIV-1 data, Table A.12 presents the mutations identified by each method for APV and SQV. Those in bold are identified in the expert panel in Rhee et al. (2006). Table A.13 presents the number of true discoveries and false discoveries of each method with respect to the expert panel. It can be seen that the proposed approach exhibits fewer false discoveries than the alternatives.

Table A.9: Analysis of the MIMIC-III data on albumin level: identified important predictors.

Identified predictors	Proposed	P-LS	DFS	LassoNet	GCRNet
Number of admissions	✓	✓	✓		
White blood cells [max]	✓	✓	✓		
Platelets [mean]	✓		✓	✓	✓
Platelets [max]	✓				
Sodium (135-148) [mean]		✓			
White blood cells (4-11,000) [max]	✓	✓	✓		
Temperature C (calc) [max]			✓		
BUN (6-20) [mean]				✓	
BUN [mean]				✓	
White blood cells from hematology [mean]				✓	
White blood cells from hematology [max]	✓	✓	✓		
Differential-Eos [mean]				✓	
Differential-laymphs	✓		✓	✓	✓
Differential-Polys		✓			

Table A.10: Analysis of the MIMIC-III data on albumin level: Frequently identified important predictors and their identification frequencies.

Identified predictors	Proposed	P-LS	DFS	LassoNet	GCRNet
Number of admissions	0.43	0.77	0.80	0.63	-
White blood cells [max]	1.00	1.00	0.90	-	-
Platelets [mean]	1.00	0.87	0.97	1.00	1.00
Platelets [max]	0.87	-	0.60	-	-
Sodium (135-148) [mean]	-	0.57	0.37	-	-
White blood cells (4-11,000) [max]	1.00	1.00	0.67	-	-
White blood cells from hematology [mean]	0.23	-	-	0.93	-
White blood cells from hematology [max]	1.00	1.00	0.93	-	-
Differential-laymphs	0.97	-	0.53	1.00	1.00

Table A.11: Analysis of the MIMIC-III data on survival: identified important predictors.

Method	Identified predictors
Proposed	Monocytes [max], Platelet Count [max], Bicarbonate [max], Arterial Blood Pressure systolic [mean], Urea Nitrogen [max], Red Blood Cells [min], Albumin [min], Paw High [min], RDW [max], Anion Gap [min], Sodium [min]
P-LS	Age, Glucose [min], Respiratory Rate [min], Lactate [mean, min], Bicarbonate [max], Anion Gap [min], Magnesium [min], pO2 [mean], Lactic Acid [min], Non Invasive Blood Pressure systolic [mean], O2 saturation pulseoxymetry [min]
DFS	-
LassoNet	Lactate [mean], O2 saturation pulseoxymetry [min], Urea Nitrogen [min], Heart Rate [min], Bicarbonate [mean, max], Arterial Blood Pressure systolic [min], Anion Gap [min], Glucose [mean], Respiratory Rate (Total) [mean], RDW [min], MCHC [max], Glucose [min], Platelet Count [max], Potassium [max]
GCRNet	-

Note: DFS is not applicable to survival data. GCRNet does not identify any predictor. Those identified by multiple methods are in bold.

Figure A.2: Analysis of the MIMIC-III data on survival: identification frequencies.

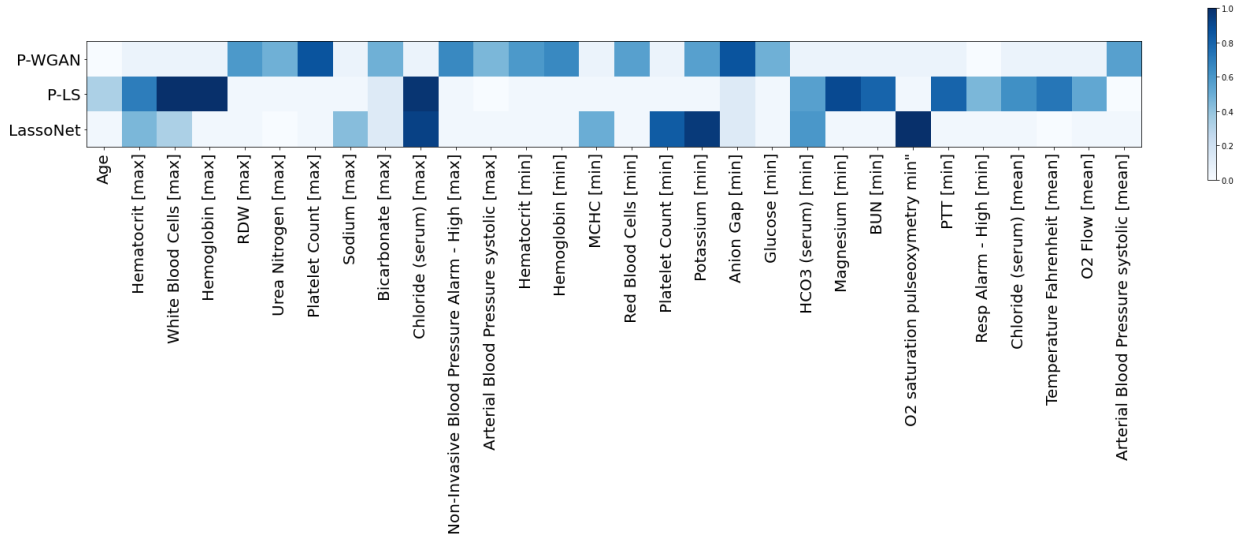


Table A.12: Analysis of the HIV dataset: identified important mutations.

Drug	Method	Identified Mutations
APV	Proposed	10F , 10I, 10V , 12Z, 20R , 20T , 33F , 43T , 46L , 47V , 48M , 48V , 50L , 50V , 54M , 64V, 71 , 82A , 82F , 84A , 84C , 84V , 88S , 90M
	P-LS	50V , 88S , 84A, 90M , 48V , 20T, 50L , 54M , 10F , 82F , 33F , 84V , 54V , 47V , 35D, 54L , 84C, 63P , 46I , 76V, 15V, 48M, 83D, 43T, 32I
	DFS	10F , 10I , 10I , 11I, 20T, 33F , 43T, 46I , 46L , 47V , 48V , 50L , 50V , 54L , 54M , 54V , 58, 76V, 82A , 82F , 84A, 84C, 84V , 88S, 90M
	LassoNet	10F , 10I , 10I , 11I, 20T, 33F , 43T, 46I , 46L , 47V , 48V , 50L , 50V , 54L , 54M , 54V , 58, 76V, 82A , 82F , 84A, 84C, 84V
	GCRNet	10F , 10I , 10I , 33F , 46I , 47V , 48M, 50L , 50V , 54M , 76V, 82A , 82F , 84A, 84V , 88S , 89V, 90M
SQV	Proposed	84A, 48V , 84C, 84V , 54S , 90M , 88D , 82F , 24I , 50L , 54T , 53L , 12P, 76V, 20I , 48M, 10I , 54V , 74S, 36I , 61D, 10F , 88S , 73S
	P-LS	84A, 48V , 84C, 90M , 84V , 48M, 88D , 76V, 53L , 54S , 10F , 50L , 54V , 67Y, 74S, 82F , 20I , 10IL, 20R , 35D, 73S , 36L , 85VI, 24I , 54T
	DFS	10F , 10IL, 20R , 24I , 35D, 48M, 48V , 50L , 53L , 54A , 54S , 54T , 54V , 58, 67Y, 73S , 74S, 76V, 82F , 84A, 84C, 84V , 88D , 88S , 90M
	LassoNet	90M , 71V , 10I , 84V , 54V , 36I , 10F , 48V , 33F , 63P , 88D , 24I , 84A, 73S , 20R , 84C, 35D, 53L , 15V, 93L , 20I , 74S, 54S , 76V, 48M
	GCRNet	10F , 10I , 10V , 13V, 24I , 35D, 36I , 36L , 41K, 46I , 48M, 48V , 53L , 54S , 54T , 54V , 62V , 63P , 64V, 67Y, 71V , 73S , 74S, 77I , 84A, 84C, 84V , 85VI , 88D , 90M , 93L

Table A.13: Analysis of the MIMIC-III data on survival: numbers of true (T) and false (F) discoveries, compared against the expert panel.

Drug	Proposed		P-LS		DFS		LassoNet		GCRNet	
	T	F	T	F	T	F	T	F	T	F
APV	19	5	16	9	17	8	16	7	14	4
SQV	17	7	16	9	15	10	18	7	21	10